Geochemical Journal, Vol. 44, pp. 1 to 22, 2010

Petrogenesis of Early Cretaceous silicic volcanism in SE Uruguay: The role of mantle and crustal sources

MICHELE LUSTRINO,[1,2]* MARIANNA MARRAZZO,[3] LEONE MELLUSO,[3] COLOMBO C. G. TASSINARI,[4] PIETRO BROTZU,[3] CELSO B. GOMES,[4] LUCIO MORBIDELLI[1] and EXCELSO RUBERTI[4]

[1]Dipartimento di Scienze della Terra, Università degli Studi di Roma La Sapienza, P.le A. Moro, 5, 00185 Roma, Italy
[2]Istituto di Geologia ambientale e Geoingegneria (IGAG, CNR), c/o Università degli Studi di Roma La Sapienza, P.le A. Moro, 5, 00185 Roma, Italy
[3]Dipartimento di Scienze della Terra, Università degli Studi di Napoli Federico II, via Mezzocannone, 8, 80134 Napoli, Italy
[4]Departamento de Mineralogia e Geotectonica, Universidade de São Paulo, Rua do Lago, 562, Cidade Universitaria, DEP 05508-900, São Paulo, Brazil

(*Received January 29, 2009; Accepted May 31, 2009*)

Early Cretaceous (~129 Ma) silicic rocks crop out in SE Uruguay between the Laguna Merín and Santa Lucía basins in the Lascano, Sierra São Miguel, Salamanca and Minas areas. They are mostly rhyolites with minor quartz-trachytes and are nearly contemporaneous with the Paraná–Etendeka igneous province and with the first stages of South Atlantic Ocean opening. A strong geochemical variability (particularly evident from Rb/Nb, Nb/Y trace element ratios) and a wide range of Sr–Nd isotopic ratios ($^{143}Nd/^{144}Nd_{(129)}$ = 0.51178–0.51209; $^{87}Sr/^{86}Sr_{(129)}$ = 0.70840–0.72417) characterize these rocks. Geochemistry allows to distinguish two compositional groups, corresponding to the north-eastern (Lascano and Sierra São Miguel, emplaced on the Neo-Proterozoic southern sector of the Dom Feliciano mobile belt) and south-eastern localities (Salamanca, Minas, emplaced on the much older (Archean) Nico Perez terrane or on the boundary between the Dom Feliciano and Nico Perez terranes). These compositional differences between the two groups are explained by variable mantle source and crust contributions. The origin of the silicic magmas is best explained by complex processes involving assimilation and fractional crystallization and mixing of a basaltic magma with upper crustal lithologies, for Lascano and Sierra São Miguel rhyolites. In the Salamanca and Minas rocks genesis, a stronger contribution from lower crust is indicated.

Keywords: Uruguay, Paraná–Etendeka, rhyolite, lower crust, crustal contamination

INTRODUCTION

The studied rocks are roughly coeval with the Paraná–Etendeka–Angola igneous province rocks (~134–124 Ma; Renne *et al*., 1992, 1996; Stewart *et al*., 1996; Marzoli *et al*., 1999; Kirstein *et al*., 2000, 2001b) and their origin is presumably related to the same processes responsible for the genesis of this large igneous province (e.g., Turner *et al*., 1999). The Paraná–Etendeka–Angola igneous province falls into the definition of Large Basaltic Province (Sheth, 2007) being the outcrops essentially made up of basaltic (actually basaltic andesites) rocks, with very scarce evolved compositions (e.g., Piccirillo and Melfi, 1988; Peate, 1997). The basic to intermediate rocks crop out in the Serra Geral Formation in Brazil and the Arapey Formation in NW Uruguay, plus minor manifestations in the Kwanza basin (Angola; Marzoli *et al*., 1999). Most of the evolved rocks (essentially trachydacites to rhyolites) crop out in the southern sectors of the Paraná basin (e.g., Garland *et al*., 1995), SE Uruguay (Arequita; e.g., Kirstein *et al*., 2000) and W Namibia (Etendeka; e.g., Ewart *et al*., 1998, 2004). Plutonic Early Cretaceous evolved rocks (mostly granodiorites to granites plus fewer syenites) are even rarer and crop out only in SE Uruguay (Valle Chico complex; Lustrino *et al*., 2005) and Namibia (e.g., Schmitt *et al*., 2000; Trumbull *et al*., 2004). During Middle Jurassic–Early Cretaceous times, the Gondwana super-continent broke up causing drifting of Africa from South America along reactivated Pan-African mobile belts (e.g., Almeida *et al*., 1984, 2000; Mantovani *et al*., 1991). The continental flood basalt (CFB) emplacement, at least in the main Paraná–Etendeka province, was slightly younger than ocean spreading. The origin of the Paraná–Etendeka province has been related to the "Tristan da Cunha Plume" and its impingement below the Brazilian–South Africa lithosphere (e.g., Gallagher and Hawkesworth, 1994; White and McKenzie, 1995; Turner *et al*., 1999). This plume is supposed to represent a ther-

*Corresponding author (e-mail: michele.lustrino@uniroma1.it)

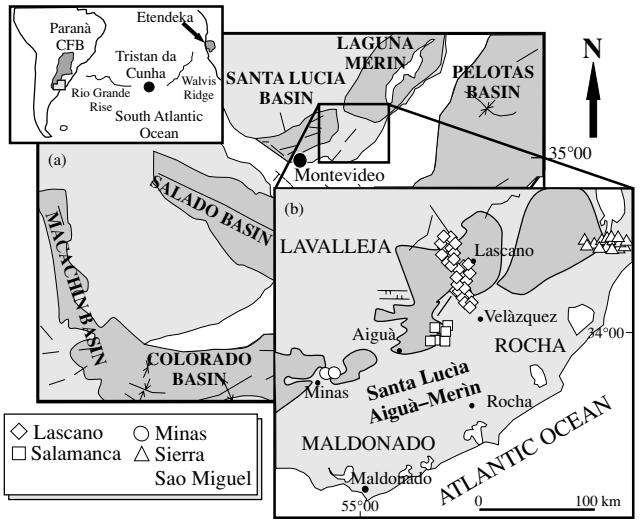

Fig. 1. (a) Structural sketch of Cretaceous basins of South America with Laguna Merín and Santa Lucía basins. In the inset are shown the "Tristan da Cunha" plume tracks, represented by the Rio Grande Rise (towards South America) and the Walvis Ridge (towards Africa), from the Archipelago of Tristan da Cunha (after O'Connor and Duncan (1990)). (b) Structural sketch-map of SE Uruguay with outcrops of Lascano, Salamanca, Sierra São Miguel and Minas rhyolites (modified after Muzio (2000)).

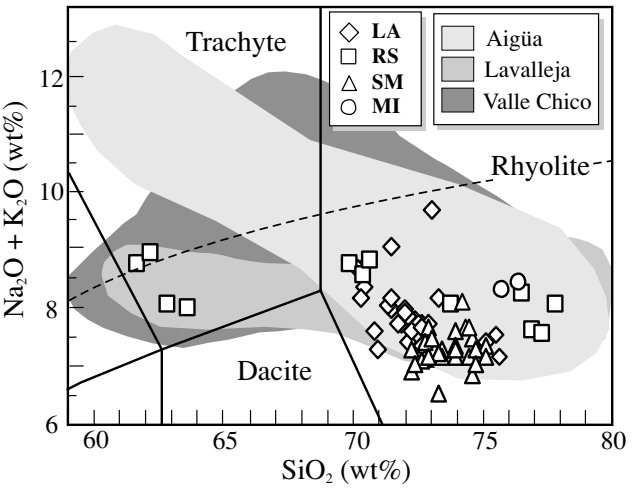

Fig. 2. TAS (total alkali vs. silica; Le Bas et al., 1986) for SE Uruguay felsic volcanics. LA, Lascano rhyolites; RS, Salamanca quartz-trachytes and rhyolites; SM, Sierra São Miguel rhyolites; MI, Minas rhyolites. Coeval silicic rocks from the same area (Lavalleja and Aigüa; Kirstein et al., 2000) and from the neighbouring Valle Chico Massif (Lustrino et al., 2005) are also shown for comparison. Dashed line: alkaline-subalkaline field division, after Irvine and Baragar (1971).

mal anomaly, whose roots would be located deep into the mantle, possibly at the core-mantle boundary. The geographic location of this mantle plume would be now centred beneath the Tristan da Cunha Archipelago in the South Atlantic. The Rio Grande Rise and Walvis Ridge in South Atlantic Ocean (Fig. 1) have been interpreted as plume tracks towards South America and Africa, respectively (e.g., O'Connor and Duncan, 1990; Muller *et al*., 1993). However, it is to note that in recent years several lines of criticism about the effective role and presence of Tristan da Cunha plume have been pointed out, and other genetic models based on trace element and isotopic data have been proposed. For example, several authors (a.o., Erlank *et al*., 1984; Piccirillo and Melfi, 1988; Marques *et al*., 1999), on the basis of incompatible trace elements and Pb isotopes, proposed old heterogeneous lithospheric mantle as the source of Paraná basalts, considering the plume only as a heat supplier necessary to partially melt the lithospheric mantle. Ernesto *et al*. (2002) proposed the involvement of delaminated sub-continental lithospheric mantle in the genesis of Paraná flood basalts and proposed the thermal anomalies present in the deep mantle as an alternative heat source.

In SE Uruguay, stretching associated with the opening of South Atlantic Ocean resulted in the formation of the Laguna Merín and Santa Lucía basins and other minor rift basins (Minas, Aigüa, Lascano and Velázquez; Veroslavsky, 1999; Fig. 1). These basins were filled by basic to intermediate magmas (basalts and basaltic andesites) of the Puerto Gomez Formation (Bossi, 1966; Kirstein *et al*., 2000; Lustrino *et al*., 2003), during an age span from ~134 to ~130 Ma (Stewart *et al*., 1996; Kirstein *et al*., 2001b). This partially overlaps in time with the emplacement of evolved rocks (mostly dacites and rhyolites) of the Arequita Formation, which have ages from ~132 to ~124 Ma (Bossi, 1966; Kirstein *et al*., 2000, 2001b). The igneous complex of Valle Chico, made up of plutonic and volcanic rocks with a predominant syenitic/trachytic composition (Muzio *et al*., 2002; Lustrino *et al*., 2005; Ruberti *et al*., 2005) is temporally and geographically associated with these volcanic rocks (Stewart *et al*., 1996; ~132 Ma; Fig. 1).

GEOLOGICAL SETTING

The Early Cretaceous magmatic rocks of SE Uruguay form scattered outcrops over an area of about 10,000 km^2 (Turner *et al*., 1999; Kirstein *et al*., 2000) between Minas and Lascano (Fig. 1), in the south-eastern edge of Paraná magmatic province. This area is underlain by a positive gravity anomaly, interpreted as an E-W oriented mafic body, whose volume is about 35,000 km^3 (Hallinan and Mantovani, unpublished data cited in Kirstein *et al*., 2000). The crystalline basement of Uruguay can be divided into three main terranes separated each other by two major shear zones with NNW-SSE (dextral) and NNE-

Table 1. Selected EMP analyses of SE Uruguayan volcanic silicic rocks feldspars, pyroxenes and opaque minerals. The complete list of the analyses can be obtained on request from the corresponding author. R, Rhyolite; Qt, Quartz-trachyte.

Sample	Rock type	SiO_2	Al_2O_3	FeO	CaO	Na_2O	K_2O	sum	*Ab*	*An*	*Or*
LA1	R	57.85	25.80	0.61	8.22	5.93	0.75	99.16	54.08	41.42	4.50
LA6	R	59.58	26.15	0.57	8.29	5.77	0.80	101.16	53.05	42.12	4.84
LA12	R	58.70	24.65	0.46	7.41	6.67	0.97	98.86	58.49	35.91	5.60
LA14	R	58.65	26.26	0.58	7.82	6.16	0.50	99.97	56.98	39.97	3.04
LA14	R	63.91	22.94	0.49	5.69	7.18	0.31	100.52	68.20	29.87	1.94
RS6	R	68.87	16.46	0.25	0.59	3.60	8.90	98.67	36.80	3.33	59.86
RS22	Qt	63.13	22.65	0.40	4.41	6.24	3.20	100.03	57.87	22.60	19.53
RS22	Qt	59.82	24.82	0.58	7.22	5.98	1.42	99.84	54.84	36.59	8.57
RS22	Qt	54.18	28.52	0.43	11.18	4.40	0.58	99.29	40.15	56.37	3.48
RS26	Qt	61.10	24.47	0.52	6.41	6.55	1.69	100.74	58.46	31.61	9.92
RS29	R	67.75	18.69	0.19	0.30	5.62	7.94	100.49	51.04	1.51	47.45
SM13	R	56.63	27.38	0.88	10.34	5.10	0.38	100.71	46.10	51.64	2.26
SM23	R	64.07	22.40	0.29	3.84	8.16	1.49	100.25	72.45	18.84	8.70
SM23	R	56.79	26.60	0.50	9.28	5.62	0.40	99.19	51.04	46.57	2.39

Sample	Rock type	SiO_2	TiO_2	Al_2O_3	FeO	MnO	MgO	CaO	Na_2O	sum	*Wo*	*Fs*	*En*
LA6	R	48.69	0.47	0.97	26.39	0.95	6.19	16.79	0.17	100.62	35.91	45.67	18.42
LA6	R	48.40	0.82	1.21	25.81	0.84	5.43	17.82	0.22	100.55	38.59	45.06	16.36
LA21	R	48.02	0.55	1.10	26.92	0.80	4.93	17.74	0.20	100.26	38.36	46.81	14.83
RS22	Qt	49.35	0.68	1.33	19.57	0.70	9.83	18.21	0.30	99.97	38.17	33.17	28.66
RS22	Qt	49.70	0.71	1.74	18.72	0.75	11.75	16.71	0.27	100.35	34.62	31.50	33.87
RS26	Qt	50.51	0.61	1.03	18.15	0.71	10.71	18.35	0.29	100.36	38.25	30.70	31.06
RS26	Qt	50.30	0.56	1.06	17.80	0.73	10.80	18.37	0.29	99.91	38.38	30.23	31.39
SM23	R	50.74	0.50	1.75	14.26	0.87	12.30	19.90	0.27	100.59	40.75	24.20	35.04
SM23	R	50.27	0.52	1.78	14.02	0.79	12.39	19.83	0.27	99.87	40.77	23.78	35.44

Sample	Rock type	TiO_2	Al_2O_3	FeO	MnO	MgO	sum	*Ilm*	*Usp*
LA6	R	17.73	1.65	71.63	0.54	0.14	91.69		0.53
LA6	R	27.87	0.92	61.74	0.78	0.22	91.53		0.84
LA14	R	50.66	0.03	45.92	1.17	0.47	98.25	0.97	
LA14	R	50.89	0.02	44.26	3.80	0.35	99.32	0.97	
LA21	R	19.99	0.91	69.78	1.24	0.05	91.97		0.60
RS22	Qt	26.50	1.62	58.66	0.77	0.98	88.53		0.82
RS22	Qt	29.35	0.99	56.59	1.32	0.97	89.22		0.91
RS26	Qt	15.60	1.53	70.55	0.69	0.08	88.45		0.48
SM13	R	21.53	1.41	66.43	0.93	0.08	90.38		0.65
SM13	R	18.95	0.95	74.40	0.91	0.01	95.22		0.55
SM23	R	1.38	0.94	90.71	0.18	0.19	93.40		0.04
SM23	R	16.60	1.63	75.07	0.73	0.09	94.12		0.63

SSW (sinistral) direction: 1) the Cuchilla–Dionisio Belt. This is known also as the Punta del Este Belt, southern part of the Dom Feliciano Belt, with Neo-Proterozoic ages ~750–600 Ma cropping out along the coast-line; 2) the Piedra Alta Terrane (~2.2–1.9 Ga) cropping out on the SW sector of Uruguay, and 3) the Nico Perez Terrane (~3.4–1.7 Ga) squeezed in between the two former terranes (Bossi, 1966; Hartmann *et al*., 2000; Basei *et al*., 2000, 2005; Bossi and Gaucher, 2004; Mallmann *et al*., 2007, and references therein). Grouped in the Nico Perez Terrane is also the Neo-Proterozoic (~590–570 Ma) calcalkaline Aigüa batholith (Fragoso Cesar *et al*., 1986). The Piedra Alta and the Nico Perez Terranes (south-western and southern Uruguay) form the oldest core of the Rio de la Plata Craton (>1.7 Ga). On the other hand, the Cuchilla–Dionisio Belt (south-eastern Uruguay) represents a much younger mobile belt belonging to the Pan-African metamorphic belt. This represents the suture zone that led to the Gondwana amalgamation during Late Proterozoic–Early Cambrian. In the south American platform this event is known as the Brasiliano cycle; Almeida *et al*., 2000; Basei *et al*., 2000, Mallmann *et al*., 2007, and references therein).

The Early Cretaceous silicic rocks studied here are

*Table 2. XRF major (wt%) and trace elements contents (ppm) of SE Uruguayan volcanic silicic rocks. R, rhyolite; Qt, Quartz-trachyte; L.O.I., Weight loss on ignition; A.S.I., Alumina Saturation Index [molar (Al_2O_3/(Na_2O + K_2O + CaO – 1.67*P_2O_5)].*

	Lascano															
Sample	LA1	LA2	LA3	LA4	LA5	LA6	LA7	LA8	LA9	LA10	LA11	LA12	LA13	LA14	LA15	LA16
Rock type	R	R	R	R	R	R	R	R	R	R	R	R	R	R	R	R
SiO_2	70.36	72.00	70.50	72.48	71.59	72.61	71.56	72.70	73.22	72.90	72.48	71.77	70.96	71.04	70.36	72.22
TiO_2	0.53	0.58	0.54	0.52	0.54	0.56	0.48	0.54	0.50	0.51	0.56	0.56	0.53	0.55	0.54	0.59
Al_2O_3	12.99	13.68	12.86	12.88	13.90	12.83	12.85	12.94	12.49	12.77	13.15	13.06	12.55	12.61	13.41	13.63
FeO_{tot}	4.84	4.83	4.88	4.72	4.35	4.65	4.75	4.63	5.06	4.87	4.84	5.41	5.16	5.10	4.99	4.96
MnO	0.09	0.09	0.08	0.24	0.03	0.10	0.08	0.10	0.03	0.03	0.04	0.20	0.09	0.10	0.07	0.25
MgO	0.16	0.52	0.37	0.29	0.07	0.60	1.00	0.37	0.48	0.16	0.20	0.31	0.30	0.46	0.35	0.44
CaO	2.61	0.74	2.32	1.29	0.63	1.48	1.48	1.23	1.20	1.23	1.09	1.18	3.00	3.11	1.86	0.67
Na_2O	2.85	2.69	2.59	3.22	3.38	2.85	3.52	3.27	2.76	3.35	3.31	3.21	3.24	2.84	3.91	2.65
K_2O	5.51	4.73	5.77	4.29	5.40	4.16	4.18	4.13	4.16	4.09	4.19	4.21	4.08	4.13	4.44	4.47
P_2O_5	0.10	0.15	0.10	0.09	0.10	0.14	0.09	0.11	0.08	0.08	0.11	0.10	0.09	0.10	0.10	0.11
Sum	100.02	99.98	100.00	100.02	100.00	99.98	100.02	100.00	100.02	100.01	100.01	100.01	100.01	100.02	100.01	99.99
L.O.I.	1.86	1.32	2.06	1.02	0.77	1.00	1.10	1.20	1.40	0.98	1.15	1.44	1.91	1.89	1.52	1.57
A.S.I.	0.85	1.28	0.88	1.06	1.12	1.10	1.00	1.08	1.12	1.06	1.11	1.10	0.83	0.86	0.92	1.33
Rb	190	191	197	171	198	163	168	171	164	157	165	165	167	173	171	178
Sr	100	96	86	119	93	116	116	134	108	119	127	130	145	136	111	126
Y	71	77	61	99	68	56	55	59	45	46	83	78	60	58	60	81
Zr	380	378	383	392	375	357	362	360	362	352	378	378	372	379	367	387
Nb	29	29	29	27	26	26	28	26	28	27	29	29	28	29	29	29
Ba	922	927	840	1180	978	840	903	1341	824	840	1005	1866	855	849	920	1486
Cr		5	5	2	3	3	7	6	7	2	3		7	4	1	0
Ni	5	10	7	9	8	5	7	9	10	4	6	6	4	5	5	10
La	52	70	50	135	68	54	51	55	47	58	108	106	54	50	59	89
Ce	105	122	98	176	119	113	99	112	109	101	137	184	103	108	110	153
Nd	51	69	52	115	58	53	49	51	45	54	104	91	53	52	56	84

	Lascano															
Sample	LA18	LA19	LA20	LA21	LA22	LA23	LA24	LA25	LA26	LA27	LA28	LA29	LA30	LA31	LA32	LA33
Rock type	R	R	R	R	R	R	R	R	R	R	R	R	R	R	R	R
SiO_2	72.83	72.69	72.58	72.18	72.29	73.07	70.61	71.51	73.00	71.57	72.77	72.10	72.08	72.70	75.43	70.48
TiO_2	0.55	0.63	0.56	0.56	0.58	0.48	0.61	0.59	0.57	0.53	0.57	0.61	0.49	0.44	0.37	0.64
Al_2O_3	13.14	12.91	12.96	12.53	13.23	11.96	13.93	14.00	13.03	13.74	12.50	13.66	13.60	13.51	12.56	14.40
FeO_{tot}	4.61	5.27	4.98	5.24	5.09	4.47	5.53	4.74	5.29	4.80	4.38	4.11	4.76	4.15	3.46	4.47
MnO	0.09	0.08	0.08	0.13	0.07	0.02	0.13	0.12	0.12	0.29	0.04	0.05	0.05	0.12	0.04	0.06
MgO	0.42	0.28	0.26	0.30	0.26	0.07	0.14	0.51	0.35	0.07	0.60	0.35	0.20	0.35	0.42	0.40
CaO	0.84	1.05	0.96	1.42	0.98	0.50	0.76	0.61	0.66	0.97	1.91	1.21	1.01	1.23	0.36	1.41
Na_2O	2.31	2.75	2.71	3.24	2.96	0.59	3.15	2.65	2.42	3.17	2.33	1.84	1.92	2.33	2.00	2.46
K_2O	5.03	4.14	4.71	4.33	4.37	8.78	4.92	5.07	4.39	4.73	4.73	5.83	5.71	5.05	5.23	5.44
P_2O_5	0.15	0.15	0.14	0.11	0.13	0.08	0.14	0.13	0.13	0.12	0.19	0.21	0.13	0.13	0.12	0.22
Sum	99.97	99.97	99.97	100.01	99.97	100.03	99.95	99.96	99.97	99.97	100.01	99.98	99.99	99.99	99.99	99.98
L.O.I.	1.25	1.25	1.01	0.81	1.25	0.76	1.06	1.37	1.66	0.83	1.14	1.18	1.37	1.47	1.47	1.60
A.S.I.	1.24	1.20	1.16	1.01	1.18	1.06	1.19	1.30	1.33	1.15	1.02	1.21	1.23	1.19	1.33	1.18
Rb	193	169	182	172	175	110	182	206	186	165	184	203	195	186	191	190
Sr	95	114	105	122	128	32	85	85	111	112	118	92	112	109	85	119
Y	91	50	70	80	51	52	70	87	77	67	57	62	78	68	67	111
Zr	372	361	383	379	373	337	386	379	371	356	399	412	484	448	380	440
Nb	29	28	26	28	27	25	29	28	27	27	23	24	28	25	22	27
Ba	1242	905	928	964	1144	631	867	1074	957	1189	1047	1106	2225	1475	1822	1595
Cr	4	7	9			6	1	6		5	11	8	4	3	6	3
Ni	4	8	4	7	6	5	4	9	8	6	9	9	11	7	4	7
La	94	68	71	65	70	42	69	77	62	56	60	74	91	69	68	78
Ce	132	121	127	124	132	92	122	139	116	107	116	132	138	142	125	149
Nd	90	68	65	60	66	43	63	67	63	57	59	64	84	65	65	81

Table 2. (continued)

	Lascano			Salamanca											
Sample	LA34	LA35	LA36	RS4	RS5	RS6	RS7	RS8	RS9	RS11	RS22	RS25	RS26	RS27	RS31
Rock type	R	R	R	R	R	R	R	R	R	R	Qt	Qt	Qt	Qt	Qt
SiO_2	75.64	75.11	73.32	76.80	76.54	73.88	70.09	70.53	77.22	77.77	62.13	62.69	63.25	63.98	70.81
TiO_2	0.34	0.33	0.36	0.21	0.22	0.36	0.50	0.47	0.19	0.21	1.41	1.40	1.35	1.39	0.47
Al_2O_3	12.77	12.90	13.89	12.60	12.74	12.86	13.96	14.38	12.24	12.11	14.89	14.88	14.34	14.17	14.66
FeO_{tot}	3.01	3.34	3.52	2.40	2.02	3.88	5.12	4.71	2.35	1.93	8.48	8.28	8.04	7.71	4.00
MnO	0.03	0.04	0.04	0.06	0.07	0.08	0.12	0.10	0.04	0.05	0.27	0.25	0.22	0.22	0.05
MgO	0.44	0.46	0.26	0.15	0.24	0.12	0.19	0.25	0.30	0.05	1.01	0.78	1.37	1.08	0.68
CaO	0.87	0.54	0.65	0.37	0.12	0.97	1.38	1.13	0.36	0.07	2.73	2.39	3.08	3.04	0.74
Na_2O	1.89	1.95	2.28	2.28	2.07	2.69	2.90	2.80	2.05	2.58	3.94	3.85	3.55	3.62	2.80
K_2O	4.96	5.19	5.60	5.05	5.88	5.08	5.55	5.43	5.22	5.18	4.49	4.81	4.18	4.06	5.69
P_2O_5	0.08	0.11	0.10	0.04	0.05	0.09	0.13	0.13	0.02	0.04	0.58	0.63	0.61	0.64	0.12
Sum	100.00	100.00	100.00	99.97	99.98	99.98	99.98	99.96	99.99	99.97	99.95	99.95	99.96	99.93	99.99
L.O.I.	1.88	1.64	1.47	0.97	1.16	1.10	1.26	1.45	1.51	1.05	1.36	1.39	1.32	1.06	1.89
A.S.I.	1.28	1.33	1.28	1.28	1.28	1.11	1.06	1.16	1.27	1.22	0.95	0.98	0.94	0.94	1.22
Rb	191	191	202	184	253	137	137	142	189	206	108	110	104	109	154
Sr	89	161	72	28	7	99	131	142	37	8	236	195	246	23	131
Y	55	60	62	65	92	59	68	69	73	56	68	77	60	55	54
Zr	366	385	397	408	704	771	1049	964	413	537	530	505	492	488	1004
Nb	22	20	23	50	88	40	43	41	49	68	54	52	48	49	41
Ba	1206	1379	1290	376	136	1309	1837	1659	431	78	1754	1760	1594	1485	2055
Cr		8	5	2	3	3	3	3		2	6	5	4	4	4
Ni	6	9	7	7	4	5	8	2	5	3	9	8	8	10	3
La	68	66	69	116	42	97	93	125	117	43	82	104	72	66	84
Ce	125	122	131	257	199	192	168	234	268	183	158	161	151	119	145
Nd	62	65	64	103	46	94	96	116	117	48	66	85	70	58	75

	Sierra São Miguel														
Sample	SM1	SM2	SM3	SM4	SM5	SM6	SM7	SM8	SM9	SM10	SM11	SM12	SM13	SM14	SM15
Rock type	R	R	R	R	R	R	R	R	R	R	R	R	R	R	R
SiO_2	72.98	72.75	72.88	73.49	74.30	73.03	72.35	73.99	74.57	73.52	73.35	72.92	73.35	72.38	74.74
TiO_2	0.59	0.67	0.62	0.60	0.50	0.57	0.58	0.62	0.63	0.67	0.63	0.67	0.67	0.69	0.54
Al_2O_3	12.25	12.30	12.12	12.29	12.31	11.94	11.83	12.41	12.29	12.39	12.43	12.23	11.18	12.14	11.84
FeO_{tot}	4.09	4.38	4.27	4.09	3.51	3.97	4.22	4.01	4.10	4.21	4.18	4.41	5.57	5.95	3.72
MnO	0.13	0.16	0.25	0.18	0.10	0.10	0.14	0.21	0.14	0.17	0.14	0.14	0.10	0.10	0.10
MgO	0.73	0.72	0.55	0.61	0.49	0.66	0.43	0.36	0.26	0.44	0.46	0.96	0.94	0.75	0.45
CaO	1.72	1.97	1.92	1.52	1.27	2.41	3.32	1.26	1.19	1.50	1.66	1.53	1.80	1.22	1.58
Na_2O	3.52	3.45	3.29	3.50	3.61	3.32	3.58	3.25	3.07	3.20	3.21	3.15	3.01	2.95	3.17
K_2O	3.82	3.35	3.86	3.48	3.76	3.87	3.44	3.64	3.51	3.65	3.69	3.73	3.24	3.65	3.70
P_2O_5	0.21	0.23	0.22	0.18	0.13	0.17	0.16	0.20	0.20	0.22	0.22	0.21	0.14	0.18	0.13
Sum	100.00	99.97	99.98	99.98	100.00	100.00	100.02	99.95	99.96	99.97	99.97	99.97	100.00	99.99	99.99
L.O.I.	0.40	0.52	0.63	0.62	0.69	1.37	1.99	0.71	0.90	0.64	0.91	0.73	1.20	1.22	0.51
A.S.I.	0.96	0.98	0.95	1.02	1.01	0.86	0.77	1.10	1.14	1.06	1.03	1.04	0.97	1.12	0.99
Rb	153	139	153	142	155	154	147	152	143	145	145	144	148	162	152
Sr	106	111	109	111	119	158	124	143	131	123	114	102	101	103	76
Y	75	71	85	64	68	69	101	78	111	81	86	68	65	95	61
Zr	345	318	348	329	332	346	369	336	359	332	339	332	322	329	316
Nb	19	19	21	19	19	20	22	20	23	22	20	19	17	19	18
Ba	752	756	787	830	801	726	711	1021	1743	945	1239	1539	607	1272	618
Cr	4	3	4		3	1		4		1	2	1	1	4	3
Ni	6	5	13	7	8	7	8	6	6	6	4	8	7	6	6
La	46	46	54	48	54	43	50	60	87	51	54	47	40	69	47
Ce	93	90	99	96	99	87	98	118	153	103	110	98	87	118	91
Nd	50	49	54	51	53	49	52	56	93	55	51	50	46	68	46

Table 2. (continued)

	Sierra São Miguel												Minas	
Sample	SM16	SM18	SM19	SM20	SM21	SM22	SM23	SM24	SM25	SM26	SM29	SM30	AQ1	AQ2
Rock type	R	R	R	R	R	R	R	R	R	R	R	R	R	R
SiO_2	74.23	73.92	75.11	73.99	74.65	74.51	72.44	73.91	74.45	74.68	75.04	74.73	76.32	75.70
TiO_2	0.57	0.55	0.50	0.50	0.51	0.56	0.61	0.53	0.49	0.53	0.55	0.57	0.22	0.18
Al_2O_3	12.29	12.34	12.28	12.11	12.38	12.51	12.28	12.93	12.33	12.08	12.21	12.75	12.33	13.60
FeO_{tot}	3.76	3.72	3.57	3.55	3.65	4.00	3.97	4.34	3.84	3.87	3.55	3.75	2.61	1.85
MnO	0.09	0.13	0.06	0.11	0.07	0.07	0.23	0.08	0.08	0.09	0.15	0.09	0.03	0.04
MgO	0.34	0.34	0.32	0.40	0.33	0.41	0.67	0.24	0.32	0.42	0.38	0.37	0.00	0.21
CaO	0.72	1.55	0.89	2.19	1.06	0.97	2.83	0.86	1.04	1.20	1.02	0.85	0.34	0.30
Na_2O	2.62	3.55	2.97	3.25	3.48	3.56	3.34	3.19	3.48	3.20	3.12	2.90	2.96	2.92
K_2O	5.21	3.73	4.11	3.79	3.70	3.27	3.43	3.78	3.90	3.80	3.76	3.83	5.17	5.11
P_2O_5	0.15	0.16	0.14	0.12	0.14	0.15	0.20	0.12	0.10	0.13	0.16	0.16	0.02	0.04
Sum	99.99	99.98	99.98	100.00	99.97	99.99	99.98	99.98	99.99	99.97	99.96	99.97	99.99	99.97
L.O.I.	0.95	0.85	0.77	1.89	0.75	1.03	1.36	0.89	0.57	0.94	0.71	1.16	0.89	0.80
A.S.I.	1.11	0.99	1.14	0.91	1.08	1.14	0.87	1.20	1.05	1.06	1.12	1.24	1.12	1.26
Rb	225	155	171	161	153	138	139	159	176	170	152	156	147	161
Sr	153	98	94	98	91	101	106	106	95	100	96	111	19	22
Y	62	94	68	84	63	92	71	83	60	68	79	114	53	53
Zr	335	353	332	358	337	355	284	403	380	384	325	343	625	411
Nb	18	21	22	22	21	20	17	25	22	24	22	23	31	35
Ba	994	785	981	756	736	1292	704	823	770	779	1104	2470	375	253
Cr	3	1	5			2	0	3	2	0	2		10	
Ni	2	7	4	6	3	4	5	3	4	5	6	8	10	4
La	42	63	55	54	51	82	44	77	50	49	63	91	82	87
Ce	83	118	92	102	82	143	91	136	94	95	103	143	173	190
Nd	47	63	53	52	54	74	50	78	54	49	60	84	77	82

Table 3(a). ICP-MS trace elements analyses (ppm) and TIMS Sr–Nd isotope data on representative SE Uruguay silicic volcanic rocks. R, Rhyolite; Qt, Quartz-trachyte.

Sample	LA9	LA12	LA34	RS6	RS9	RS22	RS26	SM9	SM13	AQ1
Rock type	R	R	R	R	R	Qt	Qt	R	R	R
Rb	141	136	163	124	155	89	93	123	132	126
Sr	112	131	92	103	36	238	253	138	106	21
Y	39	77	52	59	72	65	56	119	64	51
Zr	327	344	340	731	384	470	438	350	287	570
Nb	24	25	20	42	45	51	51	20	16	32
Sn	3.4	3.7	3.4	3.6	5.1	3.0	3.0	4.3	3.8	3.5
Cs	4.4	4.4	3.3	0.8	1.0	0.8	1.3	6.0	6.8	1.1
Ba	776	1758	1207	1321	403	1702	1562	1701	588	374
La	45.1	93.5	66.8	100.4	112.8	76.7	77.3	82.9	39.3	84.6
Ce	100.8	169.3	127.2	191.6	248.2	153.9	149.1	141.1	81.9	165.0
Pr	8.85	16.89	12.45	19.04	22.03	14.11	14.51	16.62	8.26	15.16
Nd	37.63	73.02	51.64	80.22	87.45	60.25	61.99	74.81	36.71	60.66
Sm	8.52	15.96	10.60	15.97	17.08	13.03	13.01	18.33	9.44	11.88
Eu	2.03	3.46	1.72	2.91	1.41	3.48	3.66	3.86	2.25	0.90
Gd	8.15	16.27	10.13	14.02	15.10	12.52	12.15	20.49	10.60	10.83
Tb	1.29	2.58	1.55	2.02	2.28	1.90	1.83	3.33	1.80	1.58
Dy	7.80	15.22	9.18	11.69	13.27	11.41	10.89	19.59	11.21	9.44
Ho	1.49	2.79	1.75	2.13	2.42	2.18	2.04	3.81	2.18	1.80
Er	4.85	8.31	5.39	6.59	7.50	6.64	6.19	11.44	6.81	5.66
Tm	0.75	1.23	0.79	0.97	1.14	0.98	0.88	1.65	1.01	0.88
Yb	4.86	7.70	4.90	6.10	6.93	6.15	5.80	10.04	6.32	5.25
Lu	0.69	1.09	0.70	0.86	0.96	0.90	0.84	1.45	0.92	0.76
Pb	33.4	27.4	32.1	33.9	46.6	16.7	22.4	26.1	29.7	39.1
Hf	9.33	9.73	9.98	19.24	12.35	11.47	11.37	10.10	8.71	14.94
Ta	2.18	2.30	1.71	2.50	3.24	3.76	3.67	1.78	1.51	2.21
Th	14.7	14.6	19.5	12.0	18.4	9.4	9.5	13.6	13.4	13.7
U	3.0	2.4	2.5	2.3	3.0	2.6	2.2	2.1	3.0	4.2
$^{87}Sr/^{86}Sr_{(m)}$		0.72334	0.73555		0.73737	0.71148		0.71918		0.74623
$^{143}Nd/^{144}Nd_{(m)}$		0.51221	0.51190		0.51191	0.51189		0.51199		0.51204
$^{87}Sr/^{86}Sr_{(129)}$		0.71659	0.72417		0.71019	0.70906		0.71338		0.70840
$^{143}Nd/^{144}Nd_{(129)}$		0.51209	0.51180		0.51181	0.51178		0.51186		0.51194
$\varepsilon_{Nd(129)}$		−7.3	−13.2		−12.9	−13.5		−11.9		−10.3

Table 3(b). Mass-balance calculation for SE Uruguayan silicic rocks starting from a Santa Lucía basalt-type (93L47) to quartz-trachyte (RS26) and from quartz-trachyte to rhyolites (in turn: SM9, LA34, RS7). B, basalt; Qt, Quartz-trachyte; R, rhyolite; pl, plagioclase; cpx, clinopyroxene; mt, magnetite; ap, apatite; ilm, ilmenite; Kf, K-feldspar; f, residual liquid. RS, Rio Salamanca; SM, Sierra São Miguel; LA, Lascano. Santa Lucía basalt 93L47 sample from Kirstein et al. (2000).

From	to	pl	cpx	mt	ap	ilm	ol	kf	f	$\sum R^2$
93L47 (B)	RS26 (Qt)	58.00	20.00	9.00	1.00	3.00	9.00	0.00	0.23	0.47
RS26 (Qt)	SM9 (R)	23.00	13.00	10.00	1.00	2.00	0.00	51.00	0.45	0.29
RS26 (Qt)	LA34 (R)	43.00	10.00	15.00	2.00	0.00	0.00	28.00	0.49	0.29
RS26 (Qt)	RS7 (R)	54.00	16.00	15.00	2.00	2.00	0.00	11.00	0.65	0.13

tectonically associated with important shear zones, the most important of which is the sinistral Sierra Ballena Shear Zone that connects the Nico Perez Terrane with the Cuchilla–Dionisio Belt (e.g., Mallmann *et al.*, 2007).

This paper deals with the petrographic, mineralogical, geochemical and Sr–Nd isotopic characteristics of silicic volcanic rocks of SE Uruguay and examines the role of crustal contamination in their evolution, based on a large number of whole-rock chemical analyses and mineral chemical data. The investigated rocks are essentially rhyolites, cropping out in the districts of Lascano, Salamanca, Sierra São Miguel and Minas, (SE Uruguay; Fig. 1). They form long rhyolitic ridges, usually made up of different flow units, up to 200 m thick. Occasional contacts with the underlying mafic lavas have been observed (e.g., in Salamanca and Lascano districts). The basaltic

lavas are almost exclusively known from oil industry drill holes. More frequently the silicic rocks directly overlie the Precambrian basement. The eruption mechanism responsible for the emplacement of the SE Uruguay rhyolites is still debated, being not clear if these are lava flows or rheomorphic ignimbrites (Kirstein *et al*., 2001a).

Analytical Techniques

Electron Microprobe analyses were obtained with a JEOL superprobe (15 kV; 20 mA) at the Instituto de Geociências of the University of São Paulo, Brazil and with a Cameca Camebax SX50 (15 kV; 20 mA) at the Istituto di Geologia Ambientale e Geoingegneria, CNR, Rome, Italy with full WDS procedure, using a beam size ranging from 3 μm (oxides) to 5 μm (pyroxenes) and 10 μm (feldspars) and a PAP correction method (Table 1). Major and some trace elements (Cr, Ni, Rb, Sr, Y, Zr, Nb, Ba, La, Ce and Nd) were obtained by XRF spectrometry (Philips PW 1400, Rh tube) on pressed powder pellets at the Dipartimento di Scienze della Terra, University of Trieste (Italy) following the method described in Piccirillo *et al*. (1989; Table 2). FeO was determined by colorimetry ($KMnO_4$ titration); weight loss on ignition (LOI) was measured after igniting the powder at ~900°C for 12 h, with a correction for FeO oxidation at the Dipartimento di Scienze della Terra, University of Rome La Sapienza. Selected samples were also analyzed by ICP-MS (Perkin Elmer SCIEX ELAN 6000) at Activation Laboratories (Ontario, Canada; Table 3). Precision and accuracy are reported at www.actlabs.com. Sr and Nd isotopic ratios were determined at the Geocronological Research Center of the University of São Paulo with a multicollector VG 354 Micromass (Sr) and a Finningan-MAT 262 mass spectrometer (Nd), following the methods described by Kawashita (1972) and Sato *et al*. (1995; Table 3). The Sr isotopic ratios were normalized to $^{86}Sr/^{88}Sr = 0.1194$; Nd isotopic ratios were normalized to $^{146}Nd/^{144}Nd = 0.72190$. The accuracy of measurements was checked against the NBS987 standard for Sr isotopic ratios ($^{86}Sr/^{88}Sr = 0.71028 \pm 0.00006$ in the period of the analyses) and La Jolla and BCR-1 standards for Nd isotopic ratios ($^{143}Nd/^{144}Nd = 0.511847 \pm 0.000005$; 0.512662 ± 0.000005, respectively).

Classification, Petrography and Mineral Chemistry

The silicic volcanic rocks from SE Uruguay are dominantly rhyolites according to the TAS classification of Le Bas *et al*. (1986; Fig. 2), with subordinate quartz-trachytes present only at Salamanca. Most of the SE Uruguay silicic rocks have $SiO_2 > 70$ wt%. Rocks with $SiO_2 > 78\%$ are not considered further because their extremely high SiO_2 contents may reflect a late stage alteration of the rock (silicification), which is usually associated with alkali mobility (see also discussion in Kirstein *et al*., 2000). LOI values are always <2.6 wt%. Petrographic evidence of silicification and alkali mobility are occasionally found as devetrification textures (spherulites) and secondary veins of quartz. In particular, the peraluminous character [CIPW normative corundum and A.S.I. values from 1.00 to 1.33; A.S.I. (Alumina Saturation Index) = molar $Al_2O_3/(Na_2O + K_2O + CaO - 1.76*P_2O_5)$] of some rhyolites is related to sericitization of feldspars to clay minerals. This phenomenon, coupled with silicification has been previously noted also by Kirstein *et al*. (2000), for Arequita rocks and by Lustrino *et al*. (2005), for the Valle Chico igneous complex.

The silicic volcanic rocks are essentially made up of anhydrous mineral assemblage, with plagioclase, alkali feldspar, quartz, opaque minerals, ± clinopyroxene. Among the accessory phases zircon is ubiquitous and apatite is rare. Plagioclase is the main phase in all districts, except Salamanca where sanidine phenocrysts are more abundant, both in quartz-trachytes and in rhyolites. The rare clinopyroxene has variable Fe contents: lower for Sierra São Miguel rhyolites and higher for those from Lascano (Table 1). Often this phase is transformed in secondary opaque minerals. Quartz is found also in secondary veins.

Quartz-trachytes range from vitrophyric (Porphyritic Index, P.I., 20–25%, where P.I. = area occupied by phenocrysts/total area of the thin section) to vitroclastic with isotropic texture and reddish glassy groundmass. Alkali feldspar occurs as euhedral and fractured phenocrysts (~0.5 cm), occasionally rounded and with sieve texture. Plagioclase ($Ab_{40–60}$–$An_{24–56}$–$Or_{4–16}$) occurs as anhedral normally-zoned phenocrysts, typically with anorthoclase rims ($Ab_{57–60}$–$An_{24–33}$–$Or_{9–16}$; Table 1). Locally plagioclase shows sieve texture and form star-shaped aggregates in the groundmass. Clinopyroxene is augite ($Wo_{34–38}$–$En_{28–34}$–$Fs_{30–34}$) with CaO increasing towards the rims. It occurs as interstitial microphenocrysts and/or inclusion in plagioclase. Ti–magnetite microphenocrysts (Usp content up to 94 mol%; Table 1), small equant quartz phenocrysts and microcline xenocrysts are rare constituents.

Rhyolites show a typical paragenesis made up of plagioclase, sanidine, opaque minerals, ± quartz, ± clinopyroxene. The phenocryst assemblage is set in a glassy groundmass with spherulites of opaque minerals and felted and sometimes sericitized feldspars. In Lascano, rhyolites range from porphyritic (P.I. up to 20%) to aphyric types with isotropic texture. Plagioclase phenocrysts (~0.5–1 cm) are euhedral and normally-zoned andesine/labradorite ($Ab_{48–68}$–$An_{30–53}$–$Or_{2–6}$), usually fractured with lobate margins, sometimes sericitized (Ta-

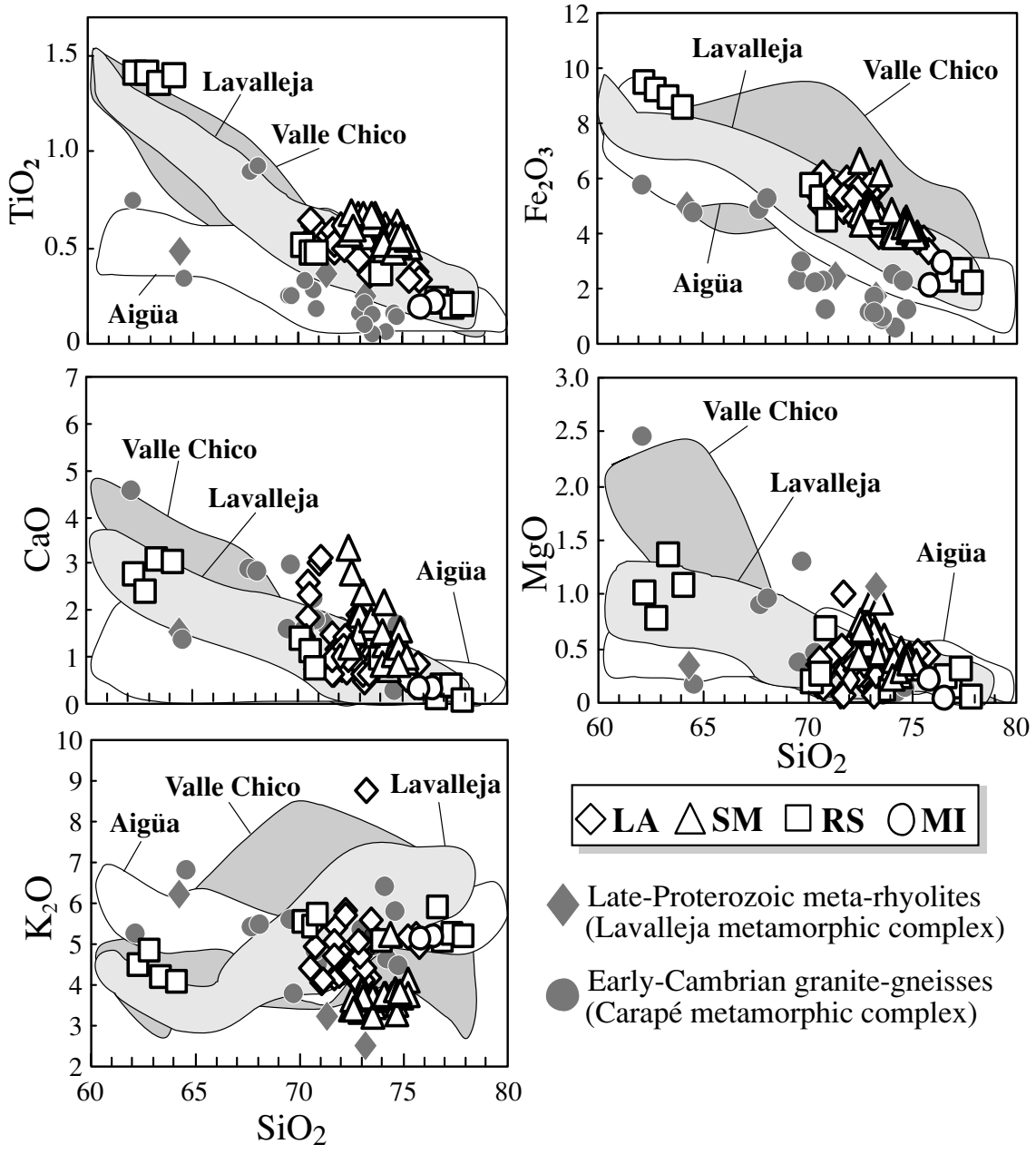

Fig. 3. Major element variation diagrams of SE Uruguayan silicic volcanic rocks. LA, Lascano rhyolites; RS, Rio Salamanca quartz-trachytes and rhyolites; SM, Sierra São Miguel rhyolites; MI, Minas rhyolites; Lavalleja, Aigüa (Kirstein et al., 2000) and Valle Chico (Lustrino et al., 2005) fields are shown for comparison. Grey diamonds, Neo-Proterozoic silicic meta-volcanic rocks of the crystalline basement (Lavalleja Formation; Sanchez Bettucci et al., 2001); Grey circles, Early Cambrian Carapé granite-gneiss complex (Sanchez Bettucci et al., 2003). See text for further explanation and geographic distribution of the plotted basement rocks.

ble 1). The minor sanidine and quartz phenocrysts show signs of partial disequilibrium with resorbed margins. Quartz also occurs in secondary veins. Opaque minerals (both Ti–magnetite and ilmenite; Usp = 41–86 mol% and Ilm ~97 mol% respectively; Table 1) and minor clinopyroxene ($Wo_{36–39}$–$En_{15–18}$–$Fs_{45–47}$; Table 1) are confined to the glassy groundmass only.

Salamanca rhyolites show several textural similarities to the Lascano silicic rocks, but the main phenocrysts are euhedral sanidine (~0.1–0.5 cm; $Ab_{37–41}$–$An_{3–5}$–$Or_{54–60}$; Table 1), occasionally with sieve texture and rounded margins, becoming more sodic in the most differentiated

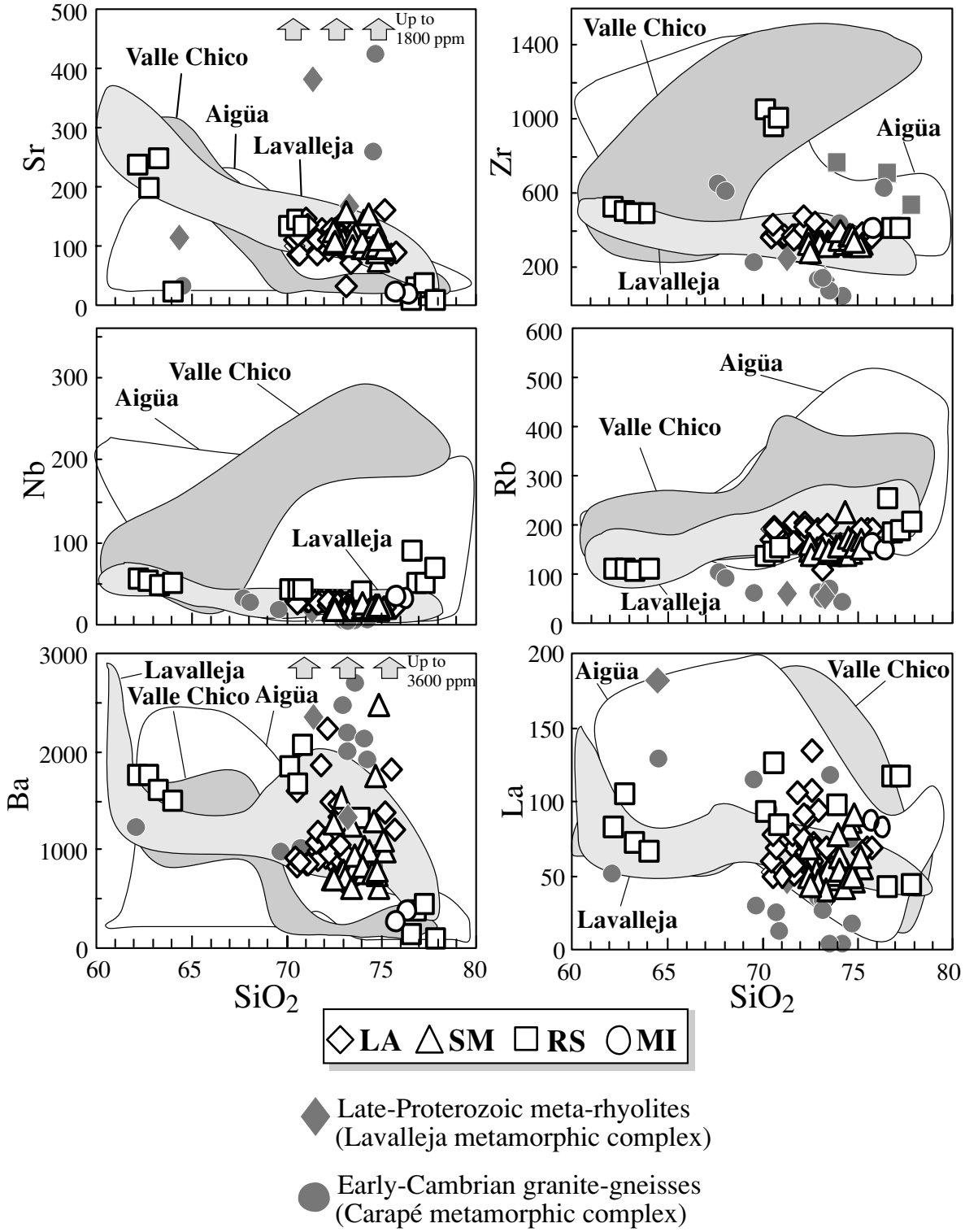

Fig. 4. Trace element variation diagrams of SE Uruguayan silicic volcanic rocks. Symbols as in Fig. 3. Lavalleja, Aigüa (Kirstein et al., 2000) and Valle Chico (Lustrino et al., 2005) fields are shown for comparison. Grey diamonds, Neo-Proterozoic silicic meta-volcanic rocks of the crystalline basement (Lavalleja Formation; Sanchez Bettucci et al., 2001); Grey circles, Early Cambrian Carapé granite-gneiss complex (Sanchez Bettucci et al., 2003). See text for further explanation and geographic distribution of the plotted basement rocks.

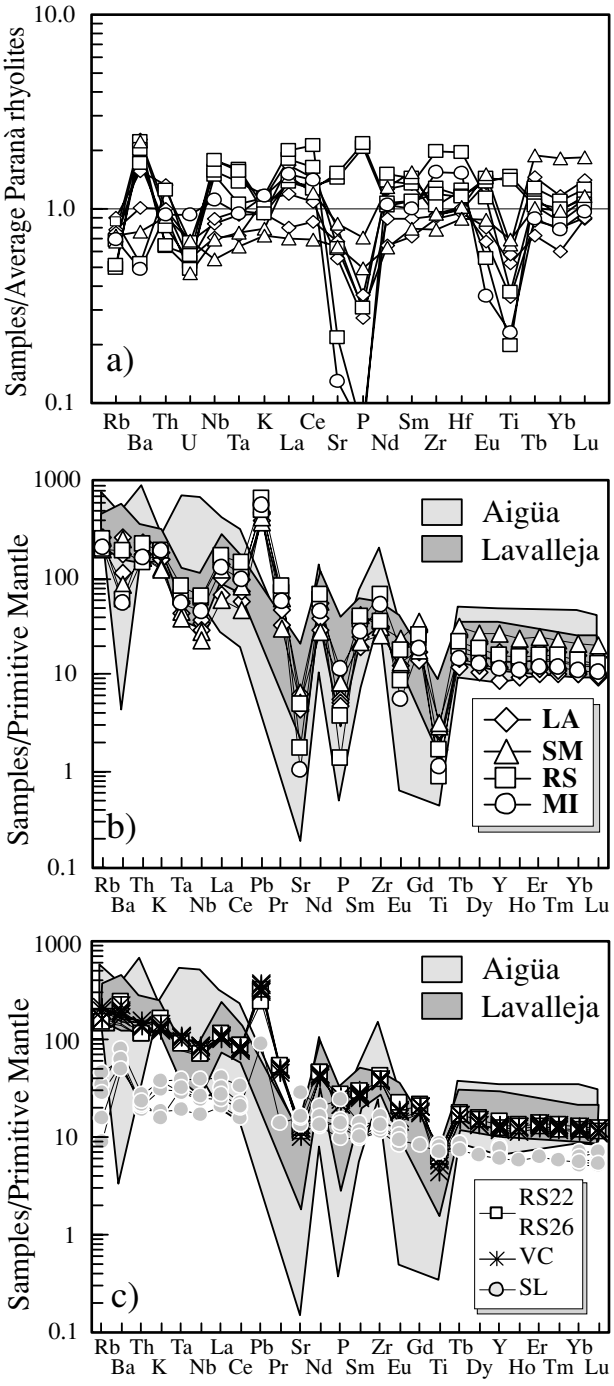

Fig. 5. (a) Incompatible trace element diagram for SE Uruguay rhyolites normalized to the average composition of the Paraná silicic rocks (both Low-Ti and High-Ti) reported by Garland et al. (1995). (b) Primitive mantle (Sun and McDonough, 1989)-normalized incompatible element diagram for SE Uruguay rhyolites. Lavalleja and Aigüa rock fields (Kirstein et al., 2000) are shown for comparison in dark grey and light grey fields, respectively. (c) Primitive mantle-normalized incompatible element diagram for the less evolved silicic rocks in SE Uruguay (RS22 and RS26; Rio Salamanca quartz-trachytes), compared to Chapecó high-Ti rhyolites (Piccirillo and Melfi, 1988; Piccirillo et al., 1989; Garland et al., 1995) and Santa Lucía-type basalts (SL; Kirstein et al., 2000). All the less evolved silicic rocks overlap and fall in the Lavalleja series field. The pattern of basalts has similar array of the quartz-trachytes but is displaced towards all incompatible elements depleted, with the exception of Sr and Ti, whose troughs in quartz-trachytes patterns are related to feldspars and Ti–magnetite fractionation. LA, Lascano rhyolites; SM, Sierra São Miguel rhyolites; RS, Rio Salamanca quartz-trachytes and rhyolites; MI, Minas rhyolites; VC, Valle Chico trachytes and quartz-trachytes (Lustrino et al., 2005); SL, Santa Lucía basalts (Kirstein et al., 2000).

rocks ($Ab_{51–55}$–An_1–$Or_{43–48}$). Minor amounts of quartz occur both as micro-phenocrysts and in secondary veins. The groundmass is clinopyroxene-free and usually glassy or fine-grained with sanidine, opaque minerals and interstitial quartz, rarely with opaque mineral spherulites, resembling type I rhyolites of Kirstein *et al*. (2000).

The Sierra São Miguel rhyolites are aphyric with an isotropic texture. Minor euhedral (0.2–0.5 cm) andesine/labradorite phenocrysts ($Ab_{46–48}$–An_{50}–Or_2) rarely show rounded margins. Groundmass plagioclase ranges from oligoclase (Ab_{72}–An_{19}–Or_9) to andesine (Ab_{51}–An_{47}–Or_2; Table 1). Opaque minerals (Ti–magnetite, with Usp up to 4 mol%; Table 1) are present as microphenocrysts (~0.3–0.4 cm) as well as groundmass phases. Quartz is present both in secondary veins and in myrmekitic intergrowth with plagioclase. The groundmass is commonly glassy. Microphenocrysts of augite are found in minor amounts. They have the highest MgO–CaO content (Wo_{41}–En_{35}–Fs_{24}) of all the augites in the districts. Fluor–apatite (F = 5.91 wt%; moderate LREE content) is found in minor amounts. These rocks resemble type II rhyolites of Kirstein *et al*. (2000).

Minas rhyolite is sub-aphyric with isotropic and hyalopilitic texture. Fractured and rounded sanidine occurs as micro-phenocrysts (~0.3 cm), usually forming clusters. Plagioclase occurs only as angular and fractured grains. Rare, rounded and fractured quartz and clinopyroxene microphenocrysts have been observed. The groundmass varies from glassy microcrystalline with little grains of quartz and feldspar and scattered microlites of opaque minerals.

Major and Trace Element Composition

Major and trace element compositions have been plotted against SiO_2 (Fig. 3). The samples fall into two distinct groups, a minor one with ~63 wt% SiO_2 (the less differentiated Rio Salamanca samples), which is separated from a larger group (>70 wt% SiO_2) by a distinct compositional gap (Table 2; Fig. 3). Overall, TiO_2, Al_2O_3, Fe_2O_3, MgO, CaO and P_2O_5 show negative correlation with SiO_2, however this correlation seems to disappear for Al_2O_3, MgO, and P_2O_5 if the low-SiO_2 samples are excluded. Among the different districts a large overlap of major and trace element content is apparent. Notwithstanding this, the Sierra São Miguel rhyolites are generally richer in TiO_2, MgO, Na_2O and P_2O_5 and poorer in K_2O than rocks of other districts at a given SiO_2, whereas Lascano rocks show a larger scatter for Al_2O_3, CaO and MgO. The distribution of trace elements versus SiO_2 is more variable. Notable are the high values of Nb and Zr for both quartz-trachytes and rhyolites of Salamanca (Nb = 40–88 ppm; Zr = 408–1049 ppm) compared to those of the other districts (Fig. 4). Sr decrease with increasing SiO_2 (from 246 to 7 ppm), while Ba shows good negative correlation with SiO_2 only for Salamanca samples.

The Paraná rhyolites, classically divided into Low-Ti (or Palmas-type) and High-Ti types (or Chapecò-type; Piccirillo and Melfi, 1988; Garland *et al*., 1995) plot in an intermediate position between the relatively low-SiO_2 and the high-SiO_2 silicic Uruguayan rocks in terms of major element content. Bearing this in mind, the silicic rocks of Uruguay have been normalized to the average composition of the Paraná silicic lavas (Garland *et al*., 1995). The Uruguayan samples show incompatible trace element content between 0.5 and 2 times the Paraná rhyolite average composition (Fig. 5a). In particular, the Salamanca rocks show the most evolved composition, with the highest content of all the incompatible trace elements and marked troughs at Sr, P and Ti. With the exception of HREE, the Sierra São Miguel samples show the lowest content of incompatible elements, while the two remaining groups (Lascano and Minas) show intermediate composition.

In primitive mantle-normalized diagram, (Fig. 5b), the rhyolites of Lascano, Salamanca, Sierra São Miguel and Minas show roughly similar patterns with marked troughs at Sr and Ti and troughs at Ta–Nb, resembling Lavallejatype rhyolites (Kirstein *et al*., 2000). The only small differences compared to Lavalleja rhyolites are the small Eu anomaly and the generally low Ba of the Lascano, Salamanca, Sierra São Miguel and Minas rhyolites, absent in the Lavalleja rocks. In Fig. 5c Salamanca quartz-trachytes show patterns surprisingly similar to Valle Chico plutonic rocks (Lustrino *et al*., 2005). The rhyolites of Sierra São Miguel and Lascano show the highest HREE content and moderate negative Eu anomalies [$(La/Yb)_N$ = 4.4–5.9; Eu/Eu* = 0.60–0.68 for Sierra São Miguel rhyolites; $(La/Yb)_N$ = 6.8–9.8; Eu/Eu* = 0.50–0.74 for Lascano rhyolites]. On the other hand, the rhyolites of Salamanca and Minas show the lowest HREE content and strong negative Eu anomalies [$(La/Yb)_N$ = 12.2 and 11.5; Eu/Eu* = 0.27 and 0.24 respectively]. Quartz-trachytes show moderate fractionated HREE [$(La/Yb)_N$ = 8.8–9.6] and slight Eu negative anomalies (Eu/Eu* = 0.83–0.88).

Sr and Nd Isotopic Data

The Sr–Nd isotopic compositions of selected samples (Table 3) have been recalculated to 129 Ma, which is the average $^{40}Ar/^{39}Ar$ age obtained by Kirstein *et al*. (2001b) for SE Uruguay silicic rocks. The acid volcanic rocks show a wide range of Sr–Nd isotopic ratios ($^{87}Sr/^{86}Sr_{(129)}$ 0.70840–0.72417; $^{143}Nd/^{144}Nd_{(129)}$ 0.51178–0.51209). In the diagram $^{143}Nd/^{144}Nd_{(129)}$ vs. $^{87}Sr/^{86}Sr$ (Fig. 7) the analyzed samples fall in an area whose vertexes are defined by three source components. One is represented by the Uruguay (Santa Lucía-type) basalts and the other two

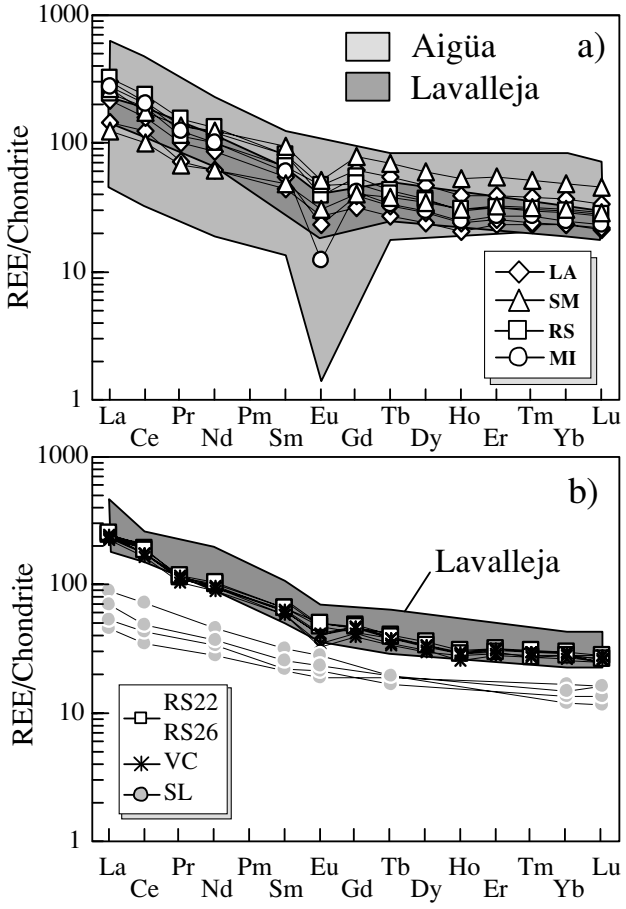

Fig. 6. (a) Chondrite-normalized REE diagram for SE Uruguay rhyolites. Lavalleja and Aigüa rock fields (Kirstein et al., 2000) are shown for comparison in dark grey and light grey fields, respectively. (b) Chondrite-normalized REE diagram for the less evolved silicic rocks in SE Uruguay (RS; Rio Salamanca), compared to Valle Chico trachytes and quartz-trachytes (Lustrino et al., 2005) and Santa Lucía-type basalts (SL; Kirstein et al., 2000). LA, Lascano; SM, Sierra São Miguel; RS, Rio Salamanca; MI, Minas; VC, Valle Chico; SL, Santa Lucía.

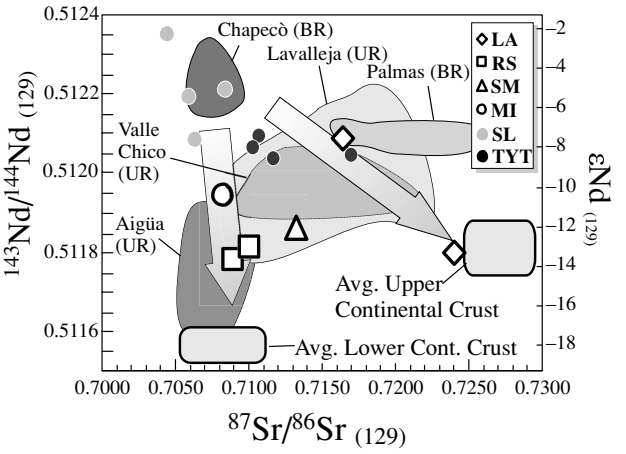

Fig. 7. $^{143}Nd/^{144}Nd_{(129)}$ vs. $^{87}Sr/^{86}Sr_{(129)}$ diagram of the rocks in SE Uruguay. The fields of Chapecó and Palmas rhyolites (Garland et al., 1995), Valle Chico complex (Lustrino et al., 2005), Aigüa and Lavalleja silicic rocks (Kirstein et al., 2000) are shown for comparison. The two grey arrows show the qualitative trends of SE Uruguay silicic rocks towards $^{143}Nd/^{144}Nd_{(129)}$ and $^{87}Sr/^{86}Sr_{(129)}$ values of upper continental crust (dark grey rectangle) and lower continental crust (light grey rectangle). LA, Lascano rhyolites; RS, Rio Salamanca quartz-trachytes and rhyolites; SM, Sierra São Miguel rhyolites; MI, Minas rhyolite. SL, Santa Lucía and Treinte Y Tres basalts (Kirstein et al., 2000).

can be qualitatively constrained to upper crust (average Proterozoic upper crustal basement; May, 1990; low ε_{Nd} and high $^{87}Sr/^{86}Sr$) and lower continental crust (average of Archean lower crustal basement; May, 1990; low ε_{Nd} and relatively low $^{87}Sr/^{86}Sr$). The Salamanca and Minas rhyolites plot near a vector connecting Santa Lucía-type basalts and average lower continental crust, whereas the Lascano rhyolites plot near a vector connecting Santa Lucía-type basalts and average upper continental crust. Sierra São Miguel rhyolite plots in intermediate position between Lascano and Salamanca rhyolites. The other two types of rhyolites previously identified in Uruguay show similar isotopic composition: the Aigüa samples cluster towards the lower crustal values in an hypothetical two-component mixing line with Santa Lucía-type basalts. The Lavalleja samples spread in a much larger isotopic area with variable amount of all the three components previously defined.

DISCUSSION

Various models have been proposed in literature to explain the origin of silicic magma in different geological contexts like continental rifting, intraplate continental and oceanic settings and destructive plate margins. As concerns the intraplate continental settings, these petrogenetic processes can be essentially resumed into two main models (e.g., Garland *et al*., 1995; Miller and Harris, 2007; Melluso *et al*., 2008, and references therein): crustal partial melting vs. fractional crystallization of a basaltic parental melt. A third option considers variable amounts of these two processes interacting at different thermo-baric conditions and volatile content (e.g., AFC-type processes).

The Lascano, Salamanca, Sierra São Miguel and Minas silicic rocks show a strong compositional variability considering the relatively small area they cover; this is particularly true for the Lascano rhyolites. On the basis of major and trace elements and mineralogical compositions, Sierra São Miguel rhyolites are considered the less

differentiated rocks, compared to the Salamanca and Minas rhyolites that show an highly differentiated character.

Partial melting process

One possibility for the origin of the silicic rocks is partial melting of local Precambrian basement or of accreted basaltic/gabbroic rocks near the Moho. Since little is known on the Uruguayan Precambrian basement, it is not possible to definitively argue for or against an involvement of these rocks as sources for the silicic rocks. South-east the city of Minas (Nico Perez Terrane), abundant Neo-Proterozoic (Pan-African; ~750–550 Ma) terranes crop out, known as the Lavalleja metamorphic complex. This formation is roughly coeval to the Brasiliano Belt in the south American continent that comprises also the Ribeira Belt (SE Brazil) and the Dom Feliciano Belt in SE Uruguay (e.g., Rogers *et al*., 1995; Almeida *et al*., 2000; Basei *et al*., 2000; Mallmann *et al*., 2007 and references therein). The Lavalleja metamorphic complex is a meta-volcanic-sedimentary sequence comprising metamorphic rocks with both sedimentary (limestone, shale, arkose, graywacke) and igneous (essentially volcanic and pyroclastic) protoliths (Sanchez Bettucci *et al*., 2001; Gaucher *et al*., 2004; Mallmann *et al*., 2007, and references therein). The bulk of the meta-igneous rocks (~80–85% of the outcrops) have a basic composition (basaltic flows and pillows, commonly metamorphosed under amphibolite facies, plus rarer meta-tuffs and meta-basaltic breccias; Sanchez Bettucci *et al*., 2001; Mallmann *et al*., 2007). The much rarer intermediate to evolved lithotypes (meta-andesites to meta-rhyolites; Sanchez Bettucci *et al*., 2001; Mallmann *et al*., 2007) crop out sporadically interlayered with chemical and clastic meta-sedimentary rocks. No geochemical data for the meta-sedimentary formations of the Lavalleja metamorphic complex are available in literature (Sanchez Bettucci, written communication, 2008).

In the Cuchilla–Dionisio Terrane, a complex puzzle of terrane has been assembled during the Brasiliano cycle: ~1 Gyr-old orthogneissic migmatites, siliciclastic meta-sedimentary cover with ~2.0–1.5 Ga MORB model-ages, plus ~0.57 Gyr-old silicic igneous rocks (both volcanic and plutonic; Mallmann *et al*., 2007, and references therein). With the possible exclusion of the migmatitic gneisses (with high solidus temperatures) these lithologies can act as potential melt source for the Early Cretaceous rocks of SE Uruguay, in particular those cropping out on the most NE-ward sectors (i.e., Lascano and Sierra São Miguel).

Other potential melt sources for the Early Cretaceous rocks of SE Uruguay are present in the Nico Perez Formation: 1) the scattered and still not fully described dioritic to granitic bodies with a rather imprecise Meso-Proterozoic age of emplacement (Bossi *et al*., 1998; Campal and Schipilov, 1999), 2) the ~1.7 Gyr-old Iliescas granite complex (N of the city of Minas; Bossi *et al*., 1998; Campal and Schipilov, 1995), 3) the Neo-Proterozoic sedimentary succession of the Arroyo del Soldato Group (pelites, limestones, sandstones and conglomerates without igneous fragments in the clastic fraction; Gaucher *et al*., 2004), 4) the Early Cambrian bimodal volcano-plutonic Sierra de las Animas Complex (with basalts and trachytes/rhyolites and plutonic equivalents, often intercalated by sedimentary successions) cropping out SW the city of Minas (Sanchez Bettucci and Rapalini, 2002; Mallmann *et al*., 2007), and 5) the Neo-Proterozoic–Early-Paleozoic Carapé granitic-gneissic complex, SE the city of Minas (Sanchez Bettucci *et al*., 2003; Mallmann *et al*., 2007). With the exception of the Carapé Granitic Complex, a detailed knowledge of the rest of the basement lithologies is missing and therefore a quantitative approach aiming to model the petrogenetic processes cannot be made. The "Carapé Granitic complex" comprises both the syn- and late- to post-orogenic granitoids, emplaced in the pre-Brasiliano basement of southern Uruguay. This complex is bounded by metamorphic rocks of Lavalleja Group, to the west, and by the Sierra Ballena Shear Zone to the east (Sanchez Bettucci *et al*., 2003).

Another possibility is that the SE Uruguay Early Cretaceous silicic rocks may be related to partial melting of coeval basaltic rocks. With regard to this option, two considerations on the volume of the basaltic rocks and their isotopic composition should be made. Differently from what observed in the rest of the Paraná basin, the area occupied by the basaltic outcrops in SE Uruguay is much smaller than the area covered by the silicic rocks. This could be considered an evidence against the hypothesis of a direct origin of the silicic rocks as partial melts of basaltic sources. However, unpublished geophysical data have detected the presence of dense bodies at upper crustal depths interpreted as gabbroic cumulates. Several lines of considerations are against the possibility of derivation of rhyolites as partial melts of cumulitic gabbroic rocks. If gabbroic cumulates are the protolith of the silicic rocks, a positive Eu/Eu* anomaly, as well as positive anomalies at Ba and Sr in primitive mantle-normalized patterns, should be expected. This is actually the opposite of what is recorded in the silicic rocks. Moreover, if the rhyolites are the partial melt of a gabbroic source, Sr–Nd isotopic similarity is expected between the two compositions. Unfortunately no isotopic data is available for this huge volume of gabbroic rocks, but we assume that the isotopic composition of the cumulates is similar to that of the rare basalt outcrops or drilled basaltic samples. Such a basaltic-rhyolitic Sr–Nd isotopic similarity has been identified in other CFB provinces (e.g., the Mozambican Lebombo rhyolites belonging to the Karoo igneous province;

Melluso *et al*., 2008) but not in SE Uruguay. SE Uruguay Early Cretaceous silicic rocks are very different from the coeval basaltic samples from a Sr–Nd isotopic point of view. Another problem regarding the origin of the SE Uruguay silicic rocks from a gabbroic source is linked to the heat necessary for the partial melting of shallow gabbroic bodies that should be very high. On these grounds a genetic link between coeval basalts (or buried gabbroic cumulates) and silicic rocks is considered unlikely.

The possibility of derivation of silicic rocks of SE Uruguay from lower crustal sources can be only qualitatively hypothesized. This is mainly based on the Sr–Nd isotopic similarity of some of the SE Uruguay silicic rocks (Minas and Salamanca) with average lower crustal lithologies, in particular for their unradiogenic Nd and mildly radiogenic Sr isotopic ratios (Fig. 7). Such a lower crustal source is not in isotopic equilibrium with basaltic outcrops or basaltic drilled samples and necessarily is not gabbroic cumulitic in composition because of the absence of Eu/Eu* positive anomalies in the silicic rocks. The high temperatures necessary to promote partial melting of such lower crustal lithologies (characterized by high solidus temperature compared to average upper crustal rocks) can be related either hypothesizing a thermal excess source (i.e., presence of mantle plume) or hypothesizing sinking of lower crustal lithologies into the hotter asthenospheric mantle after eclogitization processes. Such a delamination and detachment process of lower crustal lithologies (coupled with lithospheric mantle section) sinking into the asthenospheric mantle has been mathematically and petrologically modelled by several authors as consequence of the increase of density of eclogitic assemblages to values up to 3.8 g/cm^3, higher than average upper mantle density of ~3.3 g/cm^3 (see Lustrino, 2005 and references therein). A similar process (i.e., the presence of formerly basaltic rocks sunk down to mantle depths) has been proposed for other Paraná–Etendeka igneous rocks (e.g., the Urubici and Khumib magma types; Peate *et al*., 1999; Ewart *et al*., 2004).

Evolution processes

SE Uruguay silicic volcanic rocks follow the thermal trough between trachytic and rhyolitic minima in the petrogeny residua's system (Hamilton and MacKenzie, 1965). The same trend has been recognized for Valle Chico rocks (Lustrino *et al*., 2005) and Arequita series (Kirstein *et al*., 2000). Major and trace element variations are qualitatively consistent with a process of fractional crystallization involving feldspars, clinopyroxene and Fe–Ti–oxides, but a fractional crystallization alone, cannot explain the geochemical and isotopic features of these rocks. A process of fractional crystallization starting from a basaltic magma (Santa Lucía-type) to quartz-trachytic compositions and then from this to a rhyolitic magma has been taken into consideration, using the mass-balance calculation with the algorithm of Stormer and Nicholls (1978; Table 3b). Although major element FC-model gives acceptable results ($\sum R^2 < 1$), the Rayleigh fractionation model for the trace elements does not fit the observed compositions. Furthermore, the large variations of some incompatible trace element ratios such as Rb/Nb and Zr/Nb with SiO_2 (Figs. 8a and b), require magma evolution in an open system, which is also indicated by the wide range of Sr–Nd isotopic values (Fig. 7). The large variation involving especially alkali elements can be partly related to mobilization by secondary processes. As already evidenced, post-emplacement alteration is recorded by silicification processes, and therefore more emphasis should be put on elements that are relatively immobile in late-stage magmatic fluid systems (e.g., Zr, Ti, Nb, Th, REE). However, the concentration of these elements is strongly dependant on 1) the presence of accessory phases, 2) their stability in differentiated magmas and fluids and 3) the adopted partition coefficients. As an example, Melluso *et al*. (2008) calculated that the drop of Zr content in Mozambican rhyolites from ~1100 ppm to ~440 ppm can be accounted only for by ~0.15% fractionation of zircon. Similarly, removal of very small amount (<0.1 wt%) of monazite, apatite or other REE- or HFSE-bearing exotic phases can drastically reduce the content of these elements. Moreover, available partition coefficients of HREE in zircon in equilibrium with rhyolitic melts vary of more than one order of magnitude (e.g., Miller and Harris, 2007 and references therein). Alkali-rich silicic liquids may have very high partition coefficients for some "incompatible trace elements" (e.g., Fedele *et al*., 2009). In conclusion we believe that fractional crystallization processes had an important role in the genesis of SE Uruguay silicic rocks but other processes like variable degrees of different crustal sources and/or AFC-type processes played a major role during magmatic evolution.

The role of the local crystalline basement

It is not possible to argue for or against an important role of the local crystalline basement rocks as contaminants for the Early Cretaceous SE Uruguay melts. Anyway, a few considerations can be made. The bulk (~80–85%) of the meta-igneous rocks belonging to the Neo-Proterozoic Lavalleja Formation are basaltic (from meta-basalt to meta-gabbro with both alkaline and tholeiitic composition) and show SiO_2 content lower than 65 wt% (Sanchez Bettucci *et al*., 2001), which strongly contrasts with the much more differentiated composition of the bulk of the Early Cretaceous volcanic rocks of SE Uruguay studied here (essentially with SiO_2 higher than 70 wt%). The only (incomplete) chemical analyses reported for the

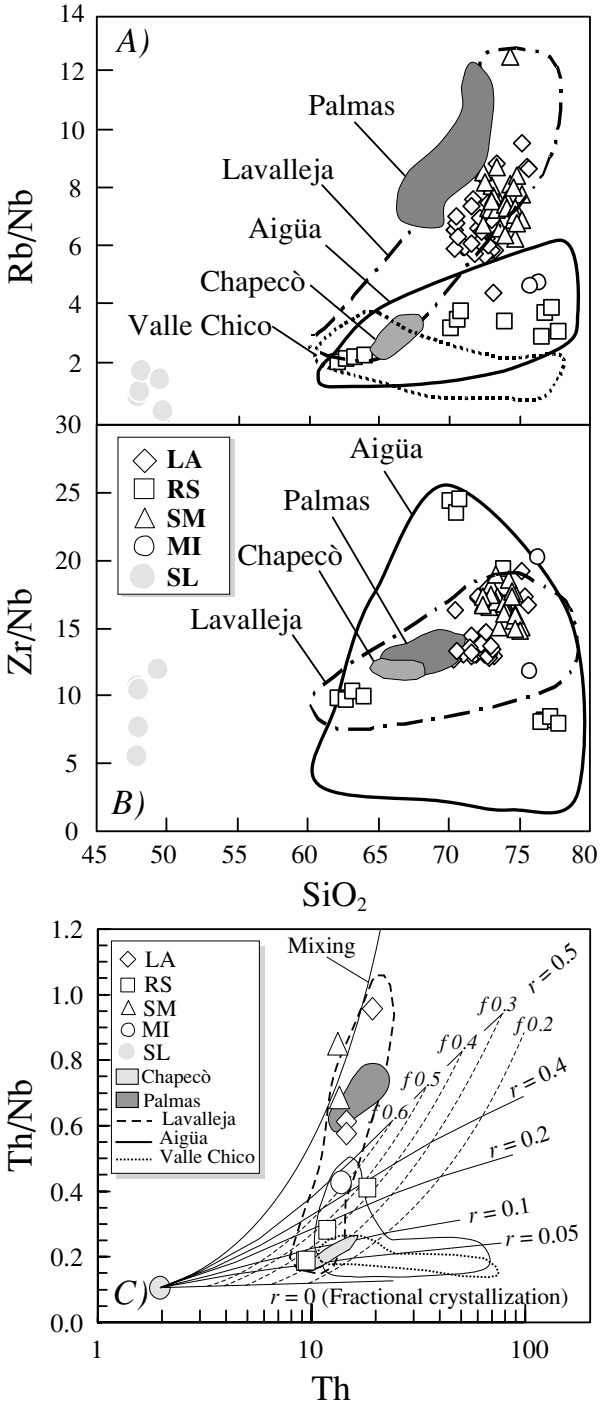

Fig. 8. (a) Plot of Rb/Nb vs. SiO_2 (wt%) for SE Uruguayan volcanic silicic rocks. Lavalleja and Aigüa series (Kirstein et al., 2000), and Valle Chico (Lustrino et al., 2005) fields are shown for comparison. In light and dark grey fields are shown Chapecó and Palmas rhyolites of Paraná, respectively (Garland et al., 1995). (b) Zr/Nb vs. SiO_2 for Lascano, Salamanca, Sierra São Miguel, Minas rhyolites compared with Lavalleja, Aigüa. Low-Ti Palmas rhyolites (Garland et al., 1995) are shown in dark grey field. LA, Lascano rhyolites; SM, Sierra São Miguel rhyolites; RS, Rio Salamanca quartz-trachytes and rhyolites; MI, Minas rhyolites; VC, Valle Chico trachytes and quartz-trachytes (Lustrino et al., 2005); SL, Santa Lucía basalts (Kirstein et al., 2000). (c) Th/Nb vs. Th of SE Uruguayan silicic rocks. For AFC model have been used D_{Nb} and D_{th} = 0.01. LA, Lascano rhyolites; SM, Sierra São Miguel rhyolites; RS, Rio Salamanca quartz-trachytes and rhyolites; AQ, Minas rhyolites; VC, Valle Chico trachytes and quartz-trachytes (Lustrino et al., 2005); SL, Santa Lucía basalts (Kirstein et al., 2000).

few (three) meta-volcanic Neo-Proterozoic rocks (rhyolites to dacites) of SE Uruguay are characterized by several geochemical characteristics (e.g., low Th/Nb ratios, low Rb, low Zr, low La) that are not compatible with an AFC-type contamination process starting from mildly evolved melts. As the SiO_2 content of the bulk of the Early Cretaceous rocks is roughly similar or higher compared to the most evolved igneous composition of the Neo-Proterozoic basement rocks of SE Uruguay, a very high *r* values in AFC-type calculation should be necessary and this is thermodynamically hard to hypothesize. Moreover, the Neoproterozoic meta-rhyolites of SE Uruguay are characterized by a much steeper REE pattern in chondrite-normalized diagrams (figure 10 of Sanchez Bettucci *et al*., 2001), lower $LREE_N$ (<200 times chondrite) and lower $HREE_N$ (<8 times chondrite), features that contrast with the less fractionated pattern of the Early Cretaceous silicic rocks of SE Uruguay (Fig. 6) and absence of fractionation between MREE and HREE (flat pattern; Fig. 6).

Another potential contaminant of the Early Cretaceous melts is the Aigüa Neoproterozoic calcalkaline batholith. Unfortunately, little is known of this terrane. It is considered as the remnant of a magmatic arc, possibly connected with the roughly coeval Pelotas and Florianopolis Batholiths to the NE (Basei *et al*., 2000, 2005). Also the Carapé Granitic Complex could be considered a potential candidate as the contaminant of SE Uruguay Early Cretaceous magmas. However, the rocks belonging to this formation show some geochemical characteristics (e.g., lower TiO_2, Fe_2O_3, Zr and Rb, and higher Sr and Ba compared to the Early Cretaceous SE Uruguay silicic rocks; Sanchez Bettucci *et al*., 2003) rendering improbable any role in the petrogenesis of the Early Cretaceous SE Uruguay silicic rocks.

To summarize, a role of the basement rocks as contaminant of the Early Cretaceous melts of SE Uruguay is not constrainable by the available geochemical data. Anyway, a role of the Precambrian basement rocks cannot be excluded because the analyses reported in literature may be not representative of the entire lithologies of the Neoproterozoic Lavalleja Formation.

AFC model and mixing

The increasing pattern of strongly incompatible/less-so-strongly incompatible element ratios with SiO_2 coupled with the troughs at Nb–Ta and positive peaks at Pb in primitive mantle-normalized diagrams, as well as the wide range of Sr–Nd isotopic ratios of SE Uruguay rhyolites suggest an involvement of crustal material in their genesis. Many authors have already recognised the effects of crustal contamination for the Lavalleja series in SE Uruguay (e.g., Turner *et al*., 1999; Kirstein *et al*., 2000), and for Gramado and Palmas rhyolites in Paraná–Etendeka Province (e.g., Piccirillo and Melfi, 1988; Piccirillo *et al*., 1989; Garland *et al*., 1995; Peate and Hawkesworth, 1996; Ewart *et al*., 1998). In other cases, Early Cretaceous silicic rocks from the Paraná–Etendeka–Angola igneous province have been considered dominantly crustal partial melts (e.g., Trumbull *et al*., 2004). Kirstein *et al*. (2000) proposed for the Lavalleja series an AFC process involving a parental Treinte Y Trés-type basaltic magma and a Brazilian leucogranite as assimilant, obtaining a rate of assimilation to fractional crystallization (r) = 0.4. Garland *et al*. (1995) used a partial melt of meta-pelitic upper crust as an assimilant to model the genesis of Palmas rhyolites in terms of AFC process starting from a Low-Ti Gramado basalt, with a $r = 0.5$. The calculation performed by Kirstein *et al*. (2000) used a geographically very far contaminant because at that time nothing was known on the geochemistry of the pre-Cambrian basement rocks of Uruguay. During the last nine years, several papers have been published on this argument and a clearer scenario is now emerging. A quantitative AFC modelling for the SE Uruguay rhyolites cannot be performed for several reasons explained above and therefore only a qualitative (or semi-quantitative) approach can be presented (Fig. 8c). The sample MAR22 (Santa Lucía-type basalt; Lustrino *et al*., 2005) has been chosen as parental melt, and Neoproterozoic granites of Maldonado area (Oyhantçabal *et al*., 2007) and a meta-rhyolite near Minas (Sanchez Bettucci *et al*., 2003) have been chosen as contaminants. The results of geochemical modelling using the three potential contaminants are nearly similar. The Th/Nb vs. Th diagram (Fig. 8c) shows AFC results using a Maldonado granite as contaminant. Salamanca quartz-trachytes cluster at ~70% fractional crystallization and $r \sim 0.05$. Salamanca rhyolites cluster at lower degrees of fractionation between 60 and 50% and r values ranging from 0.1 to 0.3, whereas Minas rhyolites plot on about 40% fractionation curve with r values ~0.4.

The AFC-type results can explain the petrogenesis of Minas and Salamanca rocks (the south-west rocks group) but fail to explain the petrogenesis of the north-eastern rhyolites (Sierra São Miguel and Lascano) because of their higher Th/Nb ratio. For these rocks an improbalby high r value (>0.5) would be required (Fig. 8c). On the other hand, a mixing process between a basaltic and a rhyolitic liquid is more reasonable. The calculated mixing curve gives a best fit for the Sierra São Miguel rhyolites (mixing with 40% granitic magma); Lascano rhyolites plot between towards higher amounts of granitic contamination. The presence of a large magmatic intrusion could easily cause partial melting of the surrounding crustal rocks (Turner *et al*., 1999).

Both upper and lower crustal contaminants seem to be involved in the genesis of SE Uruguay silicic rocks

(Fig. 7). For this reason also the rocks that seem to be characterized by a stronger lower-crustal signature have been put in the AFC scheme of Fig. 8c. The qualitative conclusions of this approach are: 1) the Sr–Nd isotope ratios furnish a definitive and valuable evidence for open system behaviour of silicic magma plumbing of SE Uruguay; 2) a three-component mixing or assimilation (basaltic melt, a lower and an upper crustal component) is involved at minimum; 3) the basaltic parental magma can be evolved up to quartz-trachytic compositions (e.g., the Rio Salamanca quartz trachytes) in a closed system and only then, at the transition between lower and upper crust, can have experienced digestion of crustal lithologies in shallower magma chambers.

Concluding Remarks

Early Cretaceous (~129 Ma) quartz trachytes and rhyolites crop out between Laguna Merín and Santa Lucía basins, in the south-eastern edge of Paraná Province. These rocks are tectonically associated with important shear zones suturing different Pan-African or older metamorphic terranes. This implies an important role of crustal anisotropies either in focusing partial melts to the surface or as protoliths of silicic melts. The main outcrop areas are at Lascano, Salamanca, Sierra São Miguel and Minas. The Lascano silicic rocks have a wide range of major and trace elements content, the Sierra São Miguel rocks show the less evolved compositions, while the Salamanca and Minas rocks are the most differentiated types.

Major element variations are qualitatively consistent with fractionation of feldspar, clinopyroxene and opaque minerals. However, the wide range of Sr–Nd initial isotopic ratios indicates AFC-type processes between a basaltic parental liquid and crustal rocks or mixing processes between a basaltic and a crust-derived partial melt at different depths. Qualitative modelling is consistent with very high degrees of r for Lascano rhyolites involving upper crustal lithologies. The absence of direct sampling (or literature data) of local upper and lower crustal lithologies has hampered a more quantitative petrogenetic approach. Neoproterozoic granitic intrusions related to the Brasiliano orogenic cycle or meta-igneous rocks of Lavalleja Group are potential candidates for upper crustal contaminant.

Low $^{143}Nd/^{144}Nd_{(129)}$ (ε_{Nd} down to –13) coupled with relatively low $^{87}Sr/^{86}Sr_{(129)}$ (down to 0.708) isotopic ratios of rocks cropping out in SE sectors (Salamanca and Minas quartz-trachytes and rhyolites) is possibly related to interaction with lower rather than upper crustal lithologies starting from Santa Lucía-type basaltic melts, thought an origin of these rocks from partial melting (~20%) of lower crust cannot be excluded. Mixing between basaltic (Santa Lucía-type) and rhyolitic melts (derived from partial melting of crustal lithologies forced to melt as consequence of the heat released by basaltic magma) is not favoured being disequilibrium paragenesis rare or absent in the Minas and Salamanca rhyolites. For the rest of rocks (Sierra São Miguel rhyolites) Sr–Nd isotopes indicate variable contribution of different components (basaltic, lower- and upper-crustal).

Acknowledgments—M.L. expresses his warm thanks to Enzo M. Piccirillo and Pino Fantauzzi (University of Trieste) for the help with XRF and the hospitality during the analytical work in Trieste. Marcello Serracino is thanked for his usual skilled assistance during EMP work. The comments of L. Kirstein (Edinburgh, UK), S. Duggen (Kiel, Germany), J. Marsh (Grahamstown, South Africa), Robert B. Trumbull (Potsdam, Germany) and two anonymous reviewers on early versions of the manuscript sensibly improved the overall quality of the work. Leda Sanchez Bettucci is thanked for her help in deciphering the complex geological evolution of Uruguay. M.L. thanks Enrica, Bianca and Laura for their patience during the writing of this manuscript and J. J. Cale for his *grasshopper*.

References

Almeida, F. F. M., Hasui, Y., De Brito Neves, B. B. and Fuck, R. A. (1984) Brazilian structural provinces: an introduction. *Earth Sci. Rev*. **17**, 1–29.

Almeida, F. F. M., De Brito Neves, B. B. and Carneiro Dal Re, C. (2000) The origin and evolution of the South American Platform. *Earth Sci. Rev*. **50**, 77–111.

Basei, M. A. S., Siga, O., Jr., Masquelin, H., Harara, O. M., Reis Neto, J. M. and Preciozzi, F. (2000) The Dom Feliciano Belt of Brazil and Uruguay and its foreland domain, the Rio de la Plata Craton: framework, tectonic evolution and correlation with similar provinces of southwestern Africa. *Tectonic Evolution of South America* (Cordani, U. G., Milani, E. J., Thomaz Filho, A. and Campos, D. A., eds.), 311–334, *31st Int. Geol. Congr*., Rio de Janeiro, Brazil.

Basei, M. A. S., Frimmel, H. E., Nutman, A. P., Preciozzi, F. and Jacob, J. (2005) A connection between the Neoproterozoic Dom Feliciano (Brazil/Uruguay) and Gariep (Namibia/South Africa) orogenic belts—evidence from a reconnaissance provenance study. *Precam. Res*. **139**, 195–221.

Bossi, J. (1966) *Geologia del Uruguay*. Dept. to de Publ. Univ. de la Repubblica, Montevideo, 460 pp.

Bossi, J. and Gaucher, C. (2004) The Cuchilla Dionisio Terrane, Uruguay: an allochtonous block accreted in the Cambrian to SW-Gondwana. *Gondwana Res*. **7**, 661–674.

Bossi, J., Ferrando, L., Montana, J., Campal, N., Morales, H., Gancio, F., Schipilov, A., Pineyro, D. and Sprechmann, P. (1998) Carta geologica del Uruguay. escala 1:500.000 Geoeditores, Montevideo, Uruguay.

Campal, N. and Schipilov, A. (1995) The Illescas luish quartz rapakivi granite (Uruguay–South America): some geological features. *Symp. Rapakivi Granites and Related Rocks*, Belém, Brazil, 18 pp.

Campal, N. and Schipilov, A. (1999) The eastern edge of the

Rio de la Plata Craton: a history of tangential collisions. *Tectonics* **13**, 33–48.

Erlank, A. J., Marsh, J. S., Duncan, A. R., Miller, R. Mc. G., Hawkesworth, C. J., Betton, P. J. and Rex, D. C. (1984) Geochemistry and petrogenesis of the Etendeka volcanic rocks from South West Africa/Namibia. *Spec. Publ. Geol. Soc. London* **13**, 195–245.

Ernesto, M., Marques, L. S., Piccirillo, E. M., Molina, E. C., Ussami, M., Comin-Chiaramonti, P. and Bellieni, G. (2002) Paraná magmatic province–Tristan da Cunha plume system: fixed versus mobile plume, petrogenetic considerations and alternative heat sources. *J. Volcanol. Geotherm. Res.* **118**, 15–36.

Ewart, A., Milner, S. C., Armstrong, R. A. and Duncan, A. R. (1998) Etendeka volcanism of the Goboboseb Mountains and Messum Igneous Complex, Namibia. Part 1: geochemical evidence of Early Cretaceous Tristan plume melts and the role of crustal contamination in the Paraná–Etendeka. *J. Petrol.* **39**, 191–225.

Ewart, A., Marsh, J. S., Milner, S. C., Duncan, A. R., Kamber, B. S. and Armstrong, R. A. (2004) Petrology and geochemistry of early Cretaceous bimodal continental flood volcanism of the NW Etendeka, Namibia. Part 1: introduction, mafic lavas and re-evaluation of mantle source components. *J. Petrol.* **45**, 59–105.

Fedele, L., Zanetti, A., Morra, V., Lustrino, M., Melluso, L. and Vannucci, R. (2009) Clinopyroxene/liquid trace element partitioning in natural trachyte-trachyphonolite systems: insights from Campi Flegrei (southern Italy). *Contrib. Mineral. Petrol.* (in press).

Fragoso Cesar, A. R. S., Figueiredo, M. C. H., Soliani, E. J. and Faccini, U. F. (1986) O batolito Pelotas (Proterozoico superior/Eopaleozoico) no Escudo do Rio Grande do Sul. *Congr. Bras. De Geol. Anais, SBG* **34** 1322–1343.

Gallagher, K. and Hawkesworth, C. (1994) Mantle plumes, continental magmatism and asymmetry in the south Atlantic. *Earth Planet. Sci. Lett.* **123**, 105–117.

Garland, F., Hawkesworth, C. J. and Mantovani, M. S. M. (1995) Description and petrogenesis of the Paraná rhyolites, Southern Brazil. *J. Petrol.* **36**, 1193–1227.

Gaucher, C., Chiglino, L. and Pecoits, E. (2004) Southernmost exposures of the Arroyo del Soldato Group (Vendian to Cambrian, Uruguay): palaeogeographic implications for the amalgamation of W-Gondwana. *Gondwana Res.* **7**, 701–714.

Hamilton, D. L. and MacKenzie, W. S. (1965) Phase-equilibrium studies in the system $NaAlSiO_4$ (nepheline)–$KAlSiO_4$ (kalsilite)–SiO_2–H_2O. *Min. Mag.* **34**, 214–231.

Hartmann, L. A., Piñeyro, D., Bossi, J., Leite, J. A. D. and McNaughton, N. J. (2000) Zircon U–Pb SHRIMP dating of Proterozoic Isla Mala granitic magmatism in the Rio de la Plata Craton, Uruguay. *J. South Am. Earth Sci.* **13**, 105–113.

Irvine, T. N. and Baragar, W. R. A. (1971) A guide to the chemical classification of the common volcanic rocks. *Can. J. Earth Sci.* **8**, 523–548.

Kawashita, K. (1972) O método Rb–Sr em rochas sedimentares. Unpublished thesis, Istituto de Geociências, USP, Brazil, 111 pp.

Kirstein, L. A., Peate, D. W., Hawkesworth, C. J., Turner, S. P., Harris, C. and Mantovani, M. S. M. (2000) Early Cretaceous basaltic and rhyolitc magmatism in Southern Uruguay associated with the opening of the South Atlantic. *J. Petrol.* **41**, 1413–1438.

Kirstein, L. A., Hawkesworth, C. J. and Garland, F. G. (2001a) Felsic lavas or rheomorphic ignimbrites: is there a chemical distinction? *Contrib. Mineral. Petrol.* **142**, 309–322.

Kirstein, L. A., Kelley. S., Hawkesworth, C., Turner, S., Mantovani, M. and Wijbrans, J. (2001b) Protracted felsic magmatic activity associated with the opening of the South Atlantic. *J. Geol. Soc. London* **158**, 583–592.

Le Bas, M. J., Le Maitre, R. W., Streckeisen, A. and Zanettin, B. (1986) A chemical classification of volcanic rocks based on the total alkali-silica diagram. *J. Petrol.* **27**, 745–750.

Lustrino, M. (2005) How the delamination and detachment of lower crust can influence basaltic magmatism. *Earth Sci. Rev.* **72**, 21–38.

Lustrino, M., Gomes, C. B., Melluso, L., Morbidelli, L., Muzio, R., Ruberti, E. and Tassinari, C. C. G. (2003) Early Cretaceous magmatic activity in SE Uruguay: trace element and Sr–Nd isotopic constraints. *IV South American Symposium on Isotope Geology*, Salvador-Ba, Brazil, August 24–27, 596–597.

Lustrino, M., Melluso, L., Brotzu, P., Gomes, C. B., Morbidelli, L., Muzio, R., Ruberti, E. and Tassinari, C. C. G. (2005) Petrogenesis of the early Cretaceous Valle Chico igneous complex (SE Uruguay): relationship with Paraná–Etendeka magmatism. *Lithos* **82**, 407–434.

Mallmann, G., Chemale, F., Jr., Avila, J. N., Kawashita, K. and Armstrong, R. A. (2007) Isotope geochemistry and geochronology of the Nico Pérez Terrane, Rio de la Plata Craton, Uruguay. *Gondwana Res.* **12**, 489–508.

Mantovani, M. S. M., Vasconelles, A. C. B. C. and Shukowsky, W. (1991) Brusque transect (SA20) from Dom Feliciano belt to the Amazon craton: explanatory pamphlet. Global Geoscience Transects Project.

Marques, L. S., Dupré, B. and Piccirillo, E. M. (1999) Mantle source compositions of the Paraná Magmatic Province (Southern Brazil): evidence from trace element and Sr–Nd–Pb isotope geochemistry. *J. Geodyn.* **28**, 439–458.

Marzoli, A., Melluso, L., Morra, V., Renne, P. R., Sgrosso, I., D'Antonio, M., Duarte Morais, L., Morais, E. A. A. and Ricci, G. (1999) Geochronology and petrology of Cretaceous basaltic magmatism in the Kwanza basin (western Angola), and relationships with the Paraná–Etendeka continental flood basalt province. *J. Geodyn.* **28**, 341–356.

May, S. E. (1990) Pan-African magmatism and regional tectonics of South Brazil. Unpublished Ph.D. Thesis, Earth Sciences, Open University.

Melluso, L., Cucciniello, C., Petrone, C. M., Lustrino, M., Morra, V., Tiepolo, M. and Vasconcelos, L. (2008). Petrology of Karoo volcanic rocks in the southern Lebombo monocline, Mozambique. *J. Afr. Earth Sci.* **52**, 139–151.

Miller, J. A. and Harris, C. (2007) Petrogenesis of the Swaziland and Northern Natal rhyolites of the Lebombo rifted margin, South East Africa. *J. Petrol.* **48**, 185–218.

Muller, R. D., Royer, J. Y. and Lawver, R. A. (1993) Revised plate motions relative to the hot spots from combined Atlantic and Indian hot spot tracks. *Geology* **21**, 275–278.

Muzio, R. (2000) Evolução petrológica e geocronologia do Maciço alcalino Valle Chico, Uruguay. Unpublished Ph.D. Thesis, IGCE-UNEPS, Rio Claro, 171 pp.

Muzio, R., Artur, A. C. and Wernik, E. (2002) Petrological and geochemical evolution of the alkaline Valle Chico Massif, southeastern Uruguay. *Int. Geol. Rev.* **44**, 352–369.

O'Connor, J. M. and Duncan, R. A. (1990) Evolution of the Walvis ridge—Rio Grande rise hot spot system. Implication for African and South American plates over plumes. *J. Geophys. Res.* **95**, 17475–17502.

Oyhantçabal, P., Siegesmund, S., Wemmer, K., Frei, R. and Layer, P. (2007) Post-collisional transition from calc-alkaline to alkaline magmatism during trascurrent deformation in the southernmost Dom Feliciano Belt (Braziliano–Pan-african, Uruguay). *Lithos* **98**, 141–159.

Peate, D. W. (1997) The Paraná–Etendeka Province. *Large Igneous Provinces: Continental, Oceanic and Planetary Flood Volcanism* (Mahoney, J. J. and Coffin, M. F., eds.), *Geophys. Mon. (AGU)* **1000**, 217–245.

Peate, D. W. and Hawkesworth, C. J. (1996) Lithospheric to asthenospheric transition in low-Ti flood basalts from southern Paraná, Brazil. *Chem. Geol.* **127**, 1–24.

Peate, D. W., Hawkesworth, C. J., Mantovani, M. M. S., Rogers, N. W. and Turner, S. P. (1999) Petrogenesis and stratigraphy of the high-Ti/U Urubici magma type in the Paraná flood basalt province and implications for the nature of "Dupal"-type mantle in the South Atlantic region. *J. Petrol.* **40**, 451–473.

Piccirillo, E. M. and Melfi, A. J. (eds.) (1988) *The Mesozoic Flood Volcanism of the Paraná Basin: Petrogenetic and Geophysical Aspects*. Instituto Astronomico e Geofisico, University of São Paulo, 600 pp.

Piccirillo, E. M., Civetta, L., Petrini, R., Longinelli, A., Bellieni, G., Comin-Chiaramonti, P., Marques, L. S. and Melfi, A. J. (1989) Regional variations within the Paraná flood basalts (southern Brazil): evidence for subcontinental mantle heterogeneity and crustal contamination. *Chem. Geol.* **75**, 103–122.

Renne, P. R., Ernesto, M., Pacca, I. G., Coe, R. S., Glen, J. M., Prévot, M. and Perrin, M. (1992) The age of Paraná flood volcanism, rifting of Gondwanaland and the Jurassic–Cretaceous boundary. *Science* **258**, 975–979.

Renne, P. R., Glen, J. M., Milner, S. C. and Duncan, A. R. (1996) Age of Etendeka flood volcanism and associated intrusions in southwestern Africa. *Geology* **24**, 659–662.

Rogers, J. J. W., Unrug, R. and Sultan, M. (1995) Tectonic assembly of Gondwana. *J. Geodyn.* **19**, 1–34.

Ruberti, E., Gomes, C. B., Tassinari, C. C. G., Antonimi, P. and Comin-Chiaramonti, P. (2005) The Early Cretaceous Valle Chico complex (Mariscala, SE Uruguay). *Mesozoic to Cenozoic Alkaline Magmatism in the Brazilian Platform* (Comin-Chiaramonti, P. and Gomes, C. B., eds.), 501–627, Editora da Universidade de São Paulo, FAPESP, São Paulo.

Sanchez Bettucci, L. and Rapalini, A. E. (2002) Paleomagnetism of the Sierra de Las Animas Complex, southern Uruguay: its implications in the assembly of western Gondwana. *Precambr. Res.* **118**, 243–265.

Sanchez Bettucci, L., Cosarinsky, M. and Ramos, V. A. (2001) Tectonic setting of the Late Proterozoic Lavalleja Group (Dom Feliciano Belt), Uruguay. *Gondwana Res.* **4**, 395–407.

Sanchez Bettucci, L., Oyhantçabal, P., Page, S. and Ramos, V. A. (2003) Petrography and geochemistry of the Carapé Granitic Complex (Southeastern Uruguay). *Gondwana Res.* **6**, 89–115.

Sato, K., Tassinari, C. G. C., Kawashita, K. and Petronillo, L. (1995) O método geocronológico Sm–Nd no IG-USP e suas aplicações. *An. Acad. Bras. Cienc.* **67**, 313–336.

Schmitt, A. K., Emmermann, R., Trumbull, R. B., Buhn, B. and Henjes-Kunst, F. (2000) Petrogenesis and $^{40}Ar/^{39}Ar$ geochronology of the Brandberg complex, Namibia: evidence for a major mantle contribution in metaluminous and peralkaline granites. *J. Petrol.* **41**, 1207–1239.

Sheth, H. (2007) 'Large Igneous Provinces (LIPs)': Definition, recommended terminology, and a hierarchical classification. *Earth Sci. Rev.* **85**, 117–124.

Stewart, K., Turner, S., Kelley, S., Hawkesworth, C., Kirstein, L. and Mantovani, M. (1996) 3-D, $^{40}Ar–^{39}Ar$ geochronology in the Paraná continental flood basalt province. *Earth Planet. Sci. Lett.* **143**, 95–109.

Stormer, J. C., Jr. and Nicholls, J. (1978) XLFRAC: a program for the interactive testing of magmatic differentiation models. *Comp. Geosci.* **4**, 143–159.

Sun, S.-S. and McDonough, W. F. (1989) Chemical and isotopic systematics of oceanic basalts. *Magmatism in the Ocean Basins* (Saunders, A. D. and Norry, M. J., eds.), *Geol. Soc. Spec. Publ.* **42**, 313–345.

Trumbull, R. B., Harris, C., Frindt, S. and Wigand, M. (2004) Oxygen and neodymium isotope evidence for source diversity in Cretaceous anorogenic granites from Namibia and implications for A-type granite genesis. *Lithos* **73**, 21–40.

Turner, S. P., Kirstein. L. A., Hawkesworth, C. J., Peate, D. W., Hallinan, S. and Mantovani, M. S. M. (1999): Petrogenesis of an 800 m lava sequence in eastern Uruguay: insights into magma chamber processes beneath the Paraná flood basalt province. *J. Geodyn.* **28**, 471–487.

Veroslavsky, G. (1999) Geologia da Bacia de Santa Lucía-Uruguai. Unpublished Ph.D. Thesis, IGCE-Unesp, Rio Claro, 152 pp.

White, R. S. and McKenzie, D. (1995) Mantle plumes and flood basalts. *J. Geophys. Res.* **100**, 543–586.